Expertise
and insight
for the future

Roosa Kokkonen and Hanna Mäntylä

Analyzing the Response of Driver Gene Targeted Drugs on *Ex Vivo* Treated Murine and Human Lung Cancer Tissue Slices

Metropolia University of Applied Sciences

Biomedical Laboratory Sciences

Bachelor of Health Care

Thesis

15.11.2019

Authors Title Number of Pages Date	Roosa Kokkonen and Hanna Mäntylä Analyzing the Response of Driver Gene Targeted Drugs on *Ex Vivo* Treated Murine and Human Lung Cancer Tissue Slices 47 pages + 5 appendices 15 November 2019
Degree	Bachelor of Health Care
Degree Programme	Biomedical Laboratory Sciences
Specialisation option	Biomedical Laboratory Sciences
Instructors	Elina Hotanen, Senior Lecturer Emmy Verschuren, FIMM-EMBL Group Leader

Worldwide the lung cancer continues being the leading cause of cancer-related mortality. By detecting the different genes involved in driving the development of lung cancer, different approaches to the treatment of lung cancer have been found. This thesis was done for the Verschuren group from the Institute for Molecular Medicine Finland (FIMM), Helsinki. The purpose of this thesis was to analyze the results of driver gene targeted drugs on murine and human lung cancer tissue slices.

We worked with murine and human lung cancer tissues, analyzed the results and collected data from the samples for the Verschuren group's later use. We had on total seven samples, four murine lung cancer samples and three human lung cancer samples. Tissues were sliced using Leica VT 1200S. Tissue slices were treated using single or combined drugs, Afatinib and Trametinib, some were treated with different concentrations and treatment times. After treatment, samples were fixed, processed, embed, sectioned and stained (H&E and IHC) according to the workflow in use in the laboratory. The stained tissue sections were scanned, and pictures processed. CL2M software was used for machine learning which was done image by image to recognize viable, dead, stromal and other cell, and background from H&E stained tissue sections.

Three of the murine samples were adenosquamous carcinoma and one adenocarcinoma. Two of the human samples were adenocarcinoma and one squamous cell carcinoma. Results differed depending on type of the tumor, treatment time and drug concentration. In some cases, combinatorial treatment seemed to be more effective and some cases single Afatinib or Trametinib treatment appeared to be more effective depending on the tumor type and whether it was human or murine sample. In some cases, further quantification needs to be done.

These results led us to the conclusion that possibly the research should be continued with human samples as the drug responses appeared to differ between human and murine lung cancer tissue slices. Of course, the number of samples tested was low therefore no further conclusions can be drawn from this thesis alone.

Keywords	lung cancer, tissue slice, driver gene, targeted drug, afatinib, trametinib

Abbreviations

AC	adenocarcinoma
AF	afatinib
Akt/ PKB	Akt serine/threonine kinase 1, protein kinase B
Ala	alanine
ASC	adenosquamous carcinoma
BRAF	*B-Raf proto-oncogene serine/threonine kinase*
CC3	cleaved caspase-3
DAB	3,3α-diaminobenzidine tetrahydrochloride
DMSO	dimethyl sulfoxide
DNA	deoxyribonucleic acid
EDTA	ethylenediaminetetraacetic acid
EGFR	*epidermal growth factor receptor*
ERBB2/ HER2	*erb-b2 receptor tyrosine kinase 2*
ERK1/2	extracellular signal-regulated kinases 1 (p44) and 2 (p42)
FDA	Food and Drug Administration
FFPE	formalin-fixed paraffin-embedded
FIMM	Institute for Molecular Medicine Finland
GEMM	genetically engineered mouse models
GTPase	guanosine-5'-triphosphate
H&E	hematoxylin and eosin
HBSS	Hanks Balanced Salt Solution
HER	*human epidermal growth factor receptor*
HRP	horseradish peroxidase
IHC	immunohistochemistry
Ki-67/ MKI67	marker of proliferation Ki-67
KL	*$Kras^{G12D/+}$; $Lkb1^{fl/fl}$*
KP	*$Kras^{G12D/+}$; $p53^{fl/fl}$*
KRAS	*Kirsten rat sarcoma viral oncogene homolog*
LCMC	Lung Cancer Mutation Consortium
LCNEC	large cell neuroendocrine carcinoma
LKB1/ STK11	*liver kinase B1, serine/threonine kinase 11*
MAPK	mitogen-activated protein kinase
mRNA	messenger ribonucleic acid

mTOR	mammalian Target of Rapamycin
NGS	next generation sequencing
NSCLC	non-small cell lung cancer
p53	*tumor protein 53*
PI3K	phosphoinositide 3-kinase
RSK	ribosomal s6 kinase
SCC	squamous cell carcinoma
SCLC	small cell lung cancer
TKI	tyrosine kinase inhibitor
TR	trametinib
Val	valine
WHO	World Health Organization

Contents

1 Introduction

Worldwide the lung cancer continues being the leading cause of cancer-related mortality. Smoking is considered as the main cause of lung cancer. However, genetic susceptibility is also associated with lung cancer as it is also discovered in non-smokers. The prognosis for lung cancer is often poor and a five-year survival rate is only about 10-13 %. (Knuuttila 2014c; Knuuttila 2014e). It is very challenging trying to cure a late stage lung cancer, since cell populations are molecularly and histologically very heterogeneous, and usually genomically unstable. Even though treatment strategies have shown promising progress in harnessing anti-tumor immunity, clinical efficacy is limited due to therapeutic resistance. Therefore, it is necessary to move into early cancer detection and prevention and thus a better understanding of the biological basis of lung cancer is required. (FIMM 2019.)

Lung cancer is characterized by its molecular changes such as mutations, translocations and amplifications. These are known as driver mutations. (Network Genomic Medicine Lung Cancer 2016.) By detecting the different genes involved in driving the development of lung cancer, different approaches to the treatment of lung cancer have been found. Many of these driver genes have already been identified. Detection of driver genes has helped for example in the development of tumor-specific agents. (Vijayalakshmi & Krishnamurthy 2011.) This has also led to the development of "Targeted Therapies" that can target therapy specifically to tumor cells (Daga et al. 2015).

We did our thesis project as part of Emmy Verschuren’s research group from the Institute for Molecular Medicine Finland (FIMM), Helsinki. In this thesis project we analyzed the response of driver gene targeted drugs on *ex vivo* treated murine and human lung cancer tissue slices. These targeted drugs specifically target the tumor cells for example by inhibiting cell growth. We worked with murine and human lung cancer tissues, treated them with single or combined drugs, then analyzed the results and collected data from the samples for the research group’s later use.

2 Lung cancer

Lung cancer has been the world's most common cancer for decades, and it continues being the leading cause of cancer-related mortality. It is the second most common cancer in men and fourth most common cancer in women. (Mali 2013a.) In Finland, there are approximately 2300 new cases of lung cancer reported annually (Knuuttila 2014e). Smoking is considered being the main cause of lung cancer, but also for example asbestos fiber, arsenic, radon, and some chromium and nickel compounds can increase the risk of lung cancer (Mali 2013c). Genetic susceptibility is also associated with lung cancer risk, but the exact mechanisms are unknown. Only some of the smokers get lung cancer and it is also found in non-smokers and in low smokers. (Knuuttila 2014c.)

The most reliable histopathological diagnosis of lung cancer is based on microscopic examination of the surgically resected tissue. If the patient is not operated, the diagnosis is based on a biopsy sample. However, the accuracy of the diagnosis from a small biopsy is not as reliable, because the tissue structure of lung cancer may vary at different sides of the tumor. Immunohistochemical stains are useful in addition to lung cancer classification and diagnosis of tumors. Immunohistochemistry (IHC) can also be used to detect for example *epidermal growth factor receptor (EGFR)* mutation, but molecular biology methods, such as gene sequencing, are still required for further classification. (Mali 2013b.)

Lung cancers are a group on heterogenous bronchial diseases, their prognosis and treatment vary on different patients (Knuuttila 2014e). The treatment is based on the type of lung cancer, spreading classification, patient's general condition and lung function, and in some cases the detection of gene mutations (Knuuttila 2014b). The TNM staging is a common way to stage the lung cancers: T (Tumor) describes the tumor penetration into its surrounding environment, N (Node) describes if the tumor is spread to the lymph nodes, and M (Metastasis) describes if the cancer has spread to a different part of the body (Knuuttila 2014a). The treatment is planned individually to each patient. Lung cancer can be treated with surgery, radiotherapy and chemotherapy, depending on the spread of cancer and condition of the patient. Different treatments are often combined. If the patient's general condition is weak, it is also possible to treat only the symptoms caused by lung cancer. (Knuuttila 2014b.)

2.1 Types of lung cancer

Lung epithelial cancers have traditionally been divided into two groups: small cell lung cancer (SCLC) and non-small cell lung cancer (NSCLC). According to World Health Organization's (WHO) classification, NSCLC is divided into three subgroups: squamous cell carcinoma (SCC), adenocarcinoma (AC), and large cell neuroendocrine carcinoma (LCNEC). (Mali 2013b.)

SCLC is a high-malignant neuroendocrine carcinoma and it is strongly associated with smoking (Knuuttila 2014d). Cells are small with nuclear molding and little cytoplasm. Cells are tightly packed, and some areas have high mitotic and apoptotic activity. SCLC tumors invade quickly and expansively to the bronchial wall and surrounding parenchyma, and they can cause compress and invasion to nearby pulmonary veins. These tumors spread typically by lymphatic and blood-borne in early stage and may secrete peptide hormones, like adrenocorticotrophic hormone and antidiuretic hormone. (Young, Stewart & O'Down 2011: 134, 139.) About 15-20% of all lung cancers are SCLC (Knuuttila 2014d).

In NSCLC, the cell morphology is bigger and has a variable number of differentiations of epithelial or glandular cells. SCC can be slowly growing, but locally invasive, and tumor necrosis is common. (Knuuttila 2014d.) Tumors arise usually in an area where squamous metaplasia appears in epithelium, following for example cigarette smoking in the main bronchi or their larger branches, close to the lung hilum (Young et al. 2011: 135). AC are the most common subtype (about 50% of the cases). Most of them originates from peripheral parts of the lung, a terminal respiratory unit. ACs are a group of histopathologically, molecularly and clinically heterogeneous diseases. (Knuuttila 2014d.) Typically, tumors format a glandular pattern and the glands are usually filled with mucus (figure 1) (Young et al. 2011: 136). The classification distinguishes three major histological groups: pre-invasive neoplasia, minimally invasive ACs and invasive ACs. LCNEC is considered being a subtype for NSCLC, but it is described as a single carcinoma in neuroendocrine tumors. It is often poorly differentiated and associated with smoking. It is the least common subtype (about 5-10 %). Tumor necrosis is possible, which is associated with poor prognosis. (Knuuttila 2014d.)

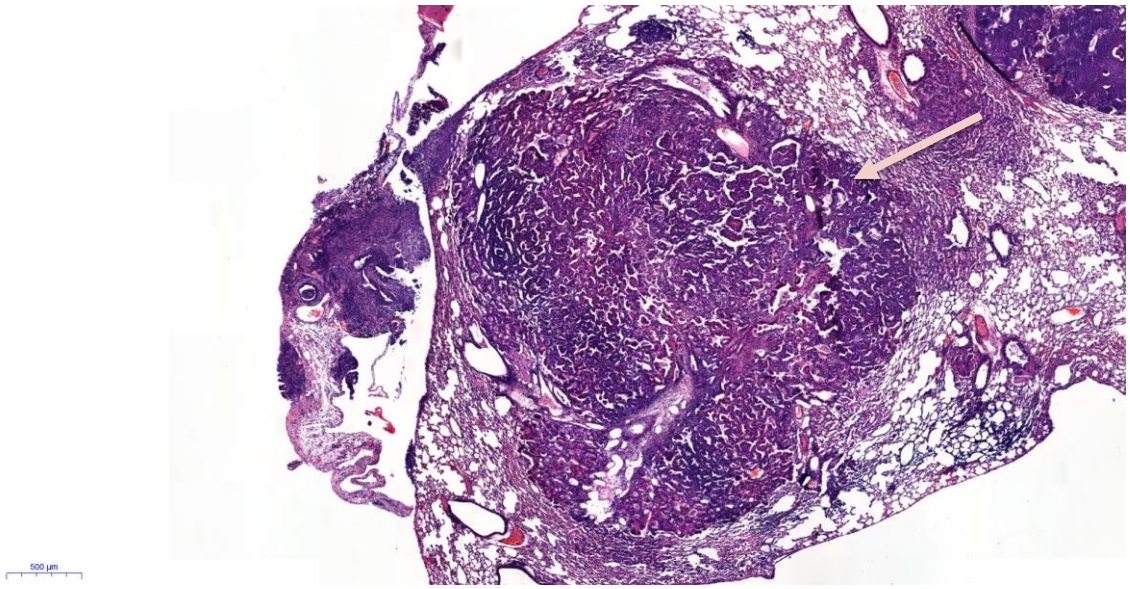

Figure 1. H&E stained adenocarcinoma (AC) area surrounding healthy murine lung tissue.

SCLC and NSCLC, and its subgroups are characterized by their molecular changes, such as mutations, translocations and amplifications. These are called driver mutations, since they are responsible for the malignant growth of the tumor cells. When more and more of these driver mutations are discovered, it allows better targeted therapy, which is more effective and better tolerated than chemotherapy. (Network Genomic Medicine Lung Cancer 2016.)

2.2 Driver mutations

Many specific genes that are participating in driving the development of lung cancer have been found. Lung Cancer Mutation Consortium (LCMC) has discovered that in almost two thirds of the advanced lung cancers have at least one of the currently known driver mutation. Advances in a molecular pathology of lung cancer have provided new strategies and tumor specific agents. Identifying these driver mutations can help in molecular targeted therapies and to guide treatment planning. Familiar and clinically relevant driver mutations in NSCLC are for example amplifications *Kirsten rat sarcoma viral oncogene homolog (KRAS)* mutation and *EGFR* mutation, and most clinically relevant translational mutations *Human epidermal growth factor receptor 2 (HER2/ERBB2)* mutation and *Akt serine/threonine kinase 1 (Akt)* mutation. (Vijayalakshmi & Krishnamurthy 2011.)

KRAS is transferase for a guanine nucleotide and it can connect intracellular signaling pathways, like mitogen-activated protein kinase pathway (MAPK), lipid kinases such as phosphoinositide 3-kinase (PI3K) and other tiny molecular weight GTPases, to cell surface receptors. Mutational *KRAS* activation leads to an aggressive cancer and often poor prognosis. (O'Hagan & Heyer 2011.) *KRAS* mutations are found in 25 % of ACs and they are the most common driver mutations in lung cancers. Different types of *KRAS* mutations have been identified and they may express themselves differently by activating different downstream signaling pathways. *KRAS* mutations can also be related with other genetic mutations for example *tumor protein p53 (p53)* or *liver kinase B1 (LKB1)*, also known as *serine/threonine kinase 11 (STK11)*. (Hirsch, Suda, Wiens & Bun 2016.) *LKB1* is a tumor suppressor gene which is usually missing from patients with NSCLC. When it comes to *KRAS* mutations chemotherapy is still the current standard of care instead of targeted drug treatment, since targeted drug treatments have been unsuccessful. (Calles et al. 2015.) *B-Raf proto-oncogene serine/tyrosine kinase (BRAF)* belongs to MAPK pathway (Baik, Myall & Wakelee 2017). *BRAF* activates the MAPK pathway and it is significant downstream signaling molecule of *KRAS*. In around 2 % of lung cancers the *BRAF* mutation is found, mostly in smokers with AC. (Hirsch et al. 2016.)

EGFR belongs to the hermaphrodite (HER) family of tyrosine kinase receptors (Hyeong, Jung, Boram & Dae 2019). EGFR activation leads to initiation of various downstream signaling pathways like Ras/Raf/MEK/MAPK and PI3K/Akt/mTOR cascades (Daga et al. 2015). These mutations are associated with never-smokers, female gender and patients with AC. NSCLC patients with *EGFR* mutations can have better prognosis when treated with *EGFR* tyrosine kinase inhibitors as primary treatment instead chemotherapy. (Hyeong et al. 2019.) Around 4-12% of *EGFR* mutations represent *EGFR* exon 20 insertion mutations. These *EGFRex20ins* mutations and their features have been analyzed by using next generation sequencing (NGS) technology. For example, *EGFR* Ala767_Val769dup mutation is most common (32,1%) of identified *EGFRex20ins* mutations. (Fang et al. 2019.) This mutation happens when the insertion of three duplicate amino acids, alanine 767 through valine 769, happens in EGFR protein kinase domain. It causes continuous phosphorylation of EGFR and downstream signaling activation. (CKB CORE 2018.)

HER2 also known as ERBB2 belongs to the HER family of receptor tyrosine kinases. HER2 causes activation of downstream signaling through Ras/MAP/MEK and PI3K/Akt pathways by forming a heterodimerizes with other receptor of HER family that may

increase oncogenic signal. (Pillai et al. 2017.) *HER2* mutation has been associated with increased metastatic potential, drug resistance and poor prognosis (Daga et al. 2015). These mutations occur only in tumors containing *KRAS* or *EGFR* mutations and they are detected mostly in female gender, non-smoking status, and patients with AC (Vijayalakshmi & Krishnamurthy 2011; Hirsch et al. 2016).

2.3 Targeted drugs used in this thesis

Driver mutations activate signaling cascades which leads to uncontrolled cell growth and proliferation. Therefore, “Targeted Therapies” has been developed. Targeted therapies are extremely specific therapeutic approach that specifically targets tumor cells. EGFR can be inhibited either by chemotherapy or by drugs, such as monoclonal antibody or small molecule tyrosine kinase inhibitors (TKI). Although at first patients treated with one of this TKIs showed good response but later ended up with disease progression. Development of *EGFR* mutation leads to structural changes which makes TKIs to lose their specificity to its binding site and causes decrease of drugs effectiveness. (Daga et al. 2015.) Also, Ras/Raf/MEK/MAPK and PI3K/Akt/mTOR pathways are alluring therapeutic targets (Hiroki et al. 2018). Afatinib (AF) inhibits cancer cells growth by binding to EGFR/ERBB1, HER2/ERBB2, or HER4/ERBB4 (National Cancer Institute 2019a). Trametinib (TR) binds to MEK 1 and 2 and inhibits growth factor-mediated cell signaling (figure 2) (National Cancer Institute 2019b). AF and TR can be diluted using for example dimethyl sulfoxide (DMSO). It is considered as a safe solvent by the Food and Drug Administration (FDA) and it is generally used as a solvent in various biomedical fields. (Verheijen et al. 2019.)

PI3K/Akt/mTOR pathway regulates cells transcription, translation, proliferation, growth, and survival. Pathway can be activated by growth factor receptors. The PI3K activation leads to phosphorylation of Akt which regulates various downstream substrates. Ras/Raf/MEK/ERK pathway regulates cell proliferation, apoptosis, migration, fate specification, and differentiation. Pathway can be activated by growth factor receptors for example EGFR. Ras protein regulates cell growth by binding to GTP which leads to Raf-1 stimulation. MEK is activated by Raf-1. MEK activation leads to activation of MAPK which activates transcription and cytoplasmic factors leading to mitogenesis. Raf-1 and MAPK are serine/thyronine kinases. (Asati, Mahapatra & Bharti 2016.) However, the inhibition of one pathway may cause other pathway activation, which lead to decrease of effectiveness of single-drug therapies (Hiroki et al. 2018).

AF is receptor tyrosine kinase EGFR family inhibitor and it has antineoplastic activity. (National Cancer Institute 2019a). It works by inhibiting cancer growth. Tyrosine kinases are proteins which stimulate cell growth. (Cancer research UK 2017.) AF irreversibly and selectively inhibits and binds to the epidermal growth factor receptors 1 (ERBB1; EGFR), 2 (ERBB2; HER2) and 4 (ERBB4; HER4) and some certain types of EGFR mutants. This might affect in the inhibition of angiogenesis and tumor growth in tumor cells which are overexpressing these receptor tyrosine kinases. (National Cancer Institute 2019a.)

TR is a kinase inhibitor and it works by preventing cancer cells to multiply (MedlinePlus 2018). It is MAPK/ERK, MEK kinase inhibitor which also have a potential antineoplastic activity. It binds to MEK 1 and 2, and acts as an inhibitor by inhibiting growth factor-mediated cell signaling and cells proliferation in several cancers. In several cancer cell types MEK 1 and 2 dual specificity to tyrosine/threonine is typically upregulated, and that is why they have a key role in regulating cell growth by activating the MEK/Ras/ERK/Raf signaling pathways. (National Cancer Institute 2019b.)

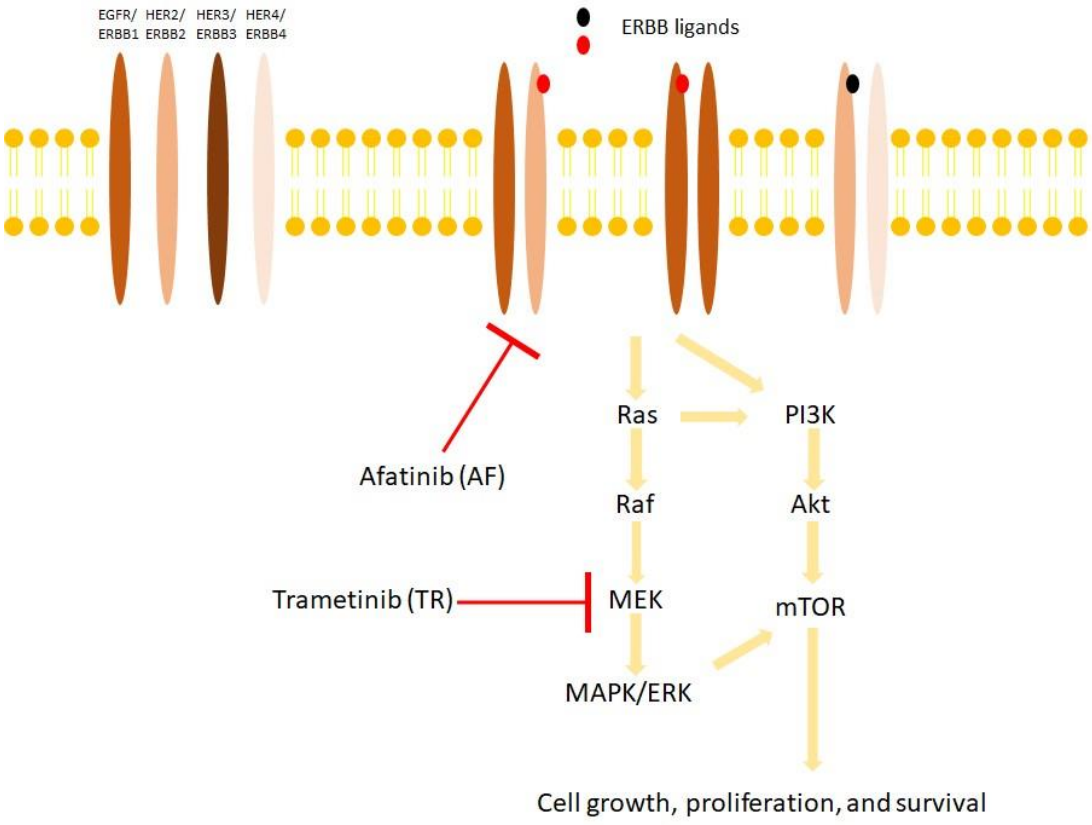

Figure 2. AF and TR inhibit Ras/Raf/MEK/ERK and PI3K/Akt/mTOR pathways (Asati, Mahapatra & Bharti 2016; National Cancer Institute 2019a; National Cancer Institute 2019b).

3 Tissue processing methods

The tissue samples entering to the laboratory are important and should be treated accordingly. Samples need to be handled safely and potential risks, such as biological and chemical hazards, should be considered prior handling the tissue samples. Every tissue sample should be labelled properly ensuring the positive identification of the tissue blocks and slides during the whole laboratory process. Preparation of the tissue samples for the histological and microscopic analysis involves many different phases. Samples are fixed, processed, embed, sectioned and stained according to the workflow in use in the laboratory. (Suvarna & Layton 2013: 95, 106.)

3.1 Fixation

The tissue samples need to be fixed prior processing. There are many different fixatives on the market, and they all have their advantages and disadvantages. Therefore, it is important to select the fixative by balancing the good aspects to the less desirable features. Most used fixative in diagnostic pathology is 10% formalin. Good fixative maintains the clear and consistent morphological features of the tissue sample. Fixative aims to preserve the tissue's cellular components, extracellular material and local chemical composition. To get a reliable view of the microanatomy and microenvironment of the tissue requires that the soluble components of the tissue are preserved during the fixation and tissue processing. When minimalizing the loss of cellular components, including DNA, mRNA, proteins, peptides and lipids, the destruction of macromolecular structures, such as mitochondria, lysosomes, and nuclear and cytoplasmic membranes, is prevented. Fixative interacts in all the phases of processing and staining. Fixation combined with tissue processing protocol produces a compromise picture of the original living tissue. (Rhodes 2013: 69-70, 73.)

3.2 Processing

Before processing, tissue blocks are placed into the right size plastic cassette. The tissue should not entirely fill the cassette. It is important to orientate the tissue in the cassette in a wanted way. (Suvarna & Layton 2013: 97-98.) The meaning of tissue processing is to remove water from the tissue and replace it with a support medium that provides adequate stiffness to enable sectioning without damaging the tissue. The first stage of processing is dehydration, where unbound water and aqueous fixatives are removed

from the tissue. Dehydration should be done slowly. Ethanol is often used in dehydration, but there are numerous dehydration mediators. After dehydration, clearing is done. Xylene is most commonly used clearing regent in histology laboratories. Clearing reagent act as a transitional between the dehydration and infiltration solutions. Tissue has a translucent appearance when the dehydration agent is completely replaced. Paraffin wax is still most used infiltration medium. It permeates the tissue in its liquid form and hardens quickly when cooled, which prevents change of the tissue structure during sectioning. Paraffin wax is suitable with most routine stains and IHC protocols. (Spencer & Bancroft 2013: 105, 107-109.)

3.3 Embedding

Embedding contains the enclosing of correctly processed and oriented sample in a support medium providing external support during the sectioning. The embedding media has to offer support for the cellular components and fill the matrix within the tissue. Paraffin wax is also most used embedding medium. Normally embedding centers consist of a cold plate, heated storage area for the cassettes and molds, and paraffin dispenser. In embedding the right size mold is chosen, the tissue is oriented in a wanted way to the mold and pressed to the bottom on the small cold plate, so the tissue stays on its place, and the cassette is attached. Paraffin wax is added to the mold on top of the tissue sample and after the cassette is attached. This produces a flat block. Mold size should be chosen so that there is enough paraffin around the tissue for support. Right orientation of the tissue sample should offer least resistance of the tissue while sectioning, and it is important for the demonstration of proper morphology. Cold plate is used to cool the paraffin block solid. (Spencer & Bancroft 2013: 110.)

3.4 Sectioning

Sectioning is the way to get the tissue samples to the glass slides, and for further microscopic examination. Most often, it is done on paraffin wax embedded tissue blocks. The basic instrument used in sectioning is the microtome. There are several types of microtomes on the market, each have a specific purpose, but many are also multifunctional. Microtome has a mechanism that moves the object, paraffin block, for an appropriate distance until it has contact with the blade. The tissue block moves vertically past the cutting blade and the tissue section is produced. (Spencer & Bancroft 2013: 125.)

The practical experience and confidence must be gained to produce quality sections. The paraffin blocks are cooled on the cold plate prior sectioning, then adjusted to the microtome. First, the tissue blocks are trimmed. Micrometer is generally set at 15-30 µm while trimming. After trimming, micrometer is generally set at 3-4 µm on routine surgical materials. Thickness depends on many factors, such as temperature, cutting speed and knife angle. When enough tissue is exposed, the tissue sections can be collected to the slide. Ideally, while sectioning the successive sections will stick on each stroke edge-to-edge due to local pressure, forming a ribbon. When a single section or a ribbon with several sections has been cut, the water bath is used for floating the tissues after sectioning. Water removes most, if not all, of the folds that occur, and tissue section flattens. The temperature of the water depends on the melting point of the paraffin wax used. Using distilled water in the water bath will prevent trapped air bubbles under the tissue sections. Single tissue sections or ribbons may now be attached onto the slide using for example a small brush (figure 3). The slide is carefully immersed into the water bath and section is floated onto the surface; so that the upper part of the section is attached. The whole tissue will stick to the slide when carefully taken out from the water bath. Excess water will disappear when the sections are dried. Drying temperature should be at the melting point of used paraffin wax. (Spencer & Bancroft 2013: 125.)

Figure 3. The tissue section can be attached to the slide for example with a small brush.

4 Histological stains

Histological staining methods are based on the physicochemical principles. Staining means the visual labeling of some biological entity, typically by attaching a color marker. The stain is the reagent or marker that is used to create the color marker. (Horobin 2013: 157.) With immunohistochemical methods certain antigen is determined by using tissue or cellular antigen (Jackson & Blythe 2013: 382; Mäkinen & Stenbäck 2012b). Stain uptake often depends on reagent-tissue or dye-tissue affinities. In this purpose, affinity describes the tendency of a stain to transfer from solution to a tissue section. The uptake of dyes and reagents is commonly multistep, and the magnitude of affinity depends on every factor used in the staining process. With stains all the interactions, such as stain-tissue, stain-solvent, and stain-stain interactions, must be considered in order to create a working staining protocol. (Horobin 2013: 157.)

Controls should be used when staining the tissue slides. Using controls help to validate the results. Especially with immunohistochemical stains, it is essential to use negative and positive control slides in order to guarantee the specificity of the used antibodies. With the negative control, the specific primary antibody is either replaced or removed from the staining protocol. It is advisable to also use positive control as the negativity of staining does not automatically mean that the antigen is not present. Positive controls have the positive elements within the test sections. (Jackson & Blythe 2013: 404.)

4.1 Rehydration and deparaffinization

Rehydration and deparaffinization needs to be done to the tissue slides before staining. Xylene is typically used in deparaffinization. Slides are washed several times with xylene, rehydrated through alcohol series with decreasing ethanol concentrations, and at the end rinsed with distilled water. (Thermo Fisher Scientific b.) Incomplete deparaffinization can have an influence on the staining result. For example, with immunohistochemical stains, paraffin wax left on the slide may interfere with the antibody's ability to penetrate the tissue, thus inhibiting antibody binding. To prevent this, the reagents used for rehydration and deparaffinization needs to be changed regularly. (Sanderson & Zardin 2013: 444.)

4.2 Hematoxylin and eosin

The hematoxylin and eosin stain (H&E) is the most commonly used histological stain. It consists of two dyes, hematoxylin and eosin. (Mäkinen 2012.) The popularity of H&E stain is based on its simplicity and ability to demonstrate clearly numerous different tissue structures (Bancroft & Layton 2013: 173). H&E stain has the advantage of a clear nuclear staining and good preservation, which is helpful assessing the degree of nuclear atypia (Mäkinen 2012).

Hematoxylin can be prepared in many ways. It is not a stain itself, but its major oxidization product, hematein can be produced from hematoxylin. Predominantly, the hematoxylin component will stain the nuclei blue-black, thus showing good intranuclear detail. Eosin stains the cell cytoplasm and extrinsic proteins such as connective tissue. The shade and intensity of an eosin stain can vary from red and pink to orange. Together, hematoxylin and eosin are very compatible to demonstrate the general histology of a tissue section. (Bancroft & Layton 2013: 173-174.) H&E staining does not stain glycogen and mucus (Mäkinen 2012).

4.3 Immunohistochemistry

IHC is a technique of which tissue or cellular antigens can be identified. Identification of antigens can be done by direct antibody labelling or by the use of secondary labelling. (Jackson & Blythe 2013: 382.) The most important use of IHC is in the detection of the origin of tumors. Used antibodies generally recognize antigens, structural proteins or secretory products, whose incidence remains stable in both benign and malignant lesions. Poor tumor differentiation does not decisively influence the staining reaction. The interpretation of good differentiation markers is usually unambiguous, either positive or negative. The second group consists of markers of cellular activity, such as proliferation markers, antigens associated with apoptosis and different stages of cell cycle. (Mäkinen & Stenbäck 2012a.)

4.3.1 Immunohistochemical methods

With the immunohistochemical methods, the presence or absence of a certain antigen is determined as precisely as possible in a tissue or cell sample. Various methods have been developed for this purpose. (Mäkinen & Stenbäck 2012b.) Direct methods are straightforward detection methods and they are based on conjugation of the primary

antibody to a label, where the tissue sample prepared is incubated with antibody-label conjugate. Since the intra-species cross reactivity is low, this labeling method does not require purification, and the use of several antibodies in a single staining procedure is permitted. With indirect methods, the sensitivity of detection is improved when a labeled secondary antibody that recognizes the primary antibody is introduced. If the used primary antibody is made in rabbit, the secondary antibody should bind to the rabbit antibody. The secondary antibody is labeled with an enzyme, such as horseradish peroxidase (HRP), which contains a polymer that reduces the background staining and increases the sensitivity of detection system. The secondary antibody and many molecules of enzyme are attached to this polymer, which makes the method simple and still maintains high sensitivity. (Jiang & McKeegan 2015: 80-81.) HRP is the most widely used enzyme label in immunohistochemical stains. It is most often used in combination with DAB (3,3α-diaminobenzidine tetrahydrochloride) chromogen, which yields a dark brown reaction end-product (figure 4). (Jackson & Blythe 2013: 385.) Due to a signal amplification, the sensitivity of indirect method is higher than direct method (Jiang & McKeegan 2015: 80-81).

Most of the immunohistochemical methods are nowadays indirect methods. Previously used methods are increasingly being displaced by so-called polymer methods, where the primary antibody sticks to the antigens on the tissue. The polymer-labeled secondary antibody recognizes the primary antibody, and the reaction is expressed by a label, peroxidase. The long polymer chain provides plenty of binding sites for the label, resulting in a strong intensity of the chromogen-induced staining reaction. The polymer methods greater sensitivity is based on the fact, that long polymer chains provide a very rich binding site for dye molecules, which results a more intense staining reaction that is easier to interpret. The advantage of the immunohistochemical methods is that the positive reaction is maintained for years and the sample preparation process can be highly automated. (Mäkinen & Stenbäck 2012b.)

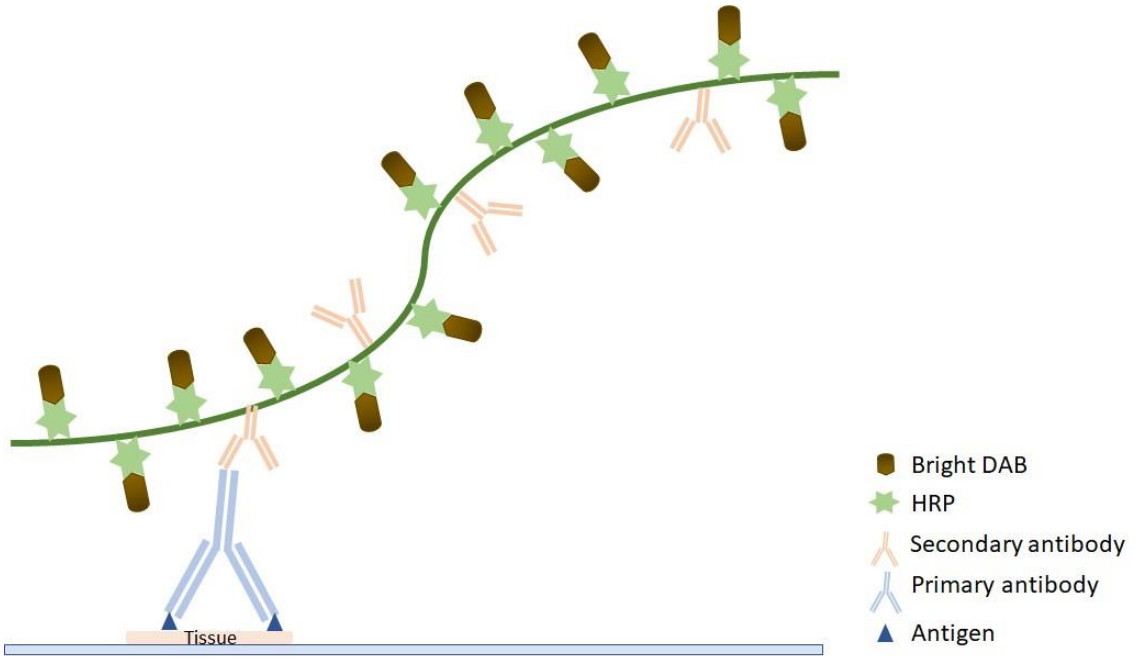

Figure 4. Indirect IHC staining protocol used in this thesis (Jackson & Blythe 2013: 385; Jiang & McKeegan 2015: 80-81).

4.3.2 Antigen retrieval

Antigen retrieval should be done before immunohistochemically staining the tissue slices. With the antigen retrieval, the effects of formalin used for fixing the tissue, can be partially reversed. (Jiang & McKeegan 2015: 77.) Intermolecular and intramolecular cross-links are formed when using formalin-based fixatives. These cross-links have certain structural proteins, which are responsible for masking the tissue antigens. There are many ways to unmask the antigen sites, and most of those have been developed for the formalin-fixed tissue material. Before antigen retrieval the tissue sections are deparaffinized and rinsed in alcohol and distilled water. (Jackson & Blythe 2013: 390-391.)

Heat-based antigen retrieval methods have improved the quality of IHC. For example, water bath can be used for antigen retrieval. The temperature of the water bath is increased below boiling point, to 95-99°C. This method has a bit longer incubation time as the temperature is not as high as in some methods, but it is gentle on the tissue and the used antigen retrieval buffer does not evaporate and can be safely reused. (Jackson & Blythe 2013: 392, 394.)

4.3.3 Blocking endogenous enzymes and background staining

Blocking endogenous enzymes prior to staining can eliminate false positive reactions. If the tissue has enzymes similar to the used antibody label, they can also react with the used substrate and thus cause problems in the interpretation of the results. Most often, the enzyme blocking is done by preincubating the sections in a solution containing hydrogen peroxide. This method does not affect to the immunoreactivity of the antigens but is has been reported to almost completely eliminate the endogenous peroxidase activity. (Jackson & Blythe 2013: 402.)

Endogenous enzyme activity and ionic interactions are the major causes of background staining. For example, non-specific antigen uptake can cause significant amount of background staining and interfere in interpretation. (Jackson & Blythe 2013: 403.) The blocking of background staining can be done with the blocking solution that contains proteins isolated from the same species in which the antibody was made in. This blocking solution prevents non-specific binding of the primary and secondary antibodies thus reducing the unwanted background staining. (Jiang & McKeegan 2015: 77.)

4.3.4 Antibodies

Antibodies to hundreds of different antigens are available for diagnostic use. The most important diagnostic group is the antibodies used in tumor diagnostics. Other indications are e.g. forecast markers that includes for example antibodies showing proliferation and mutations in oncogenes or growth inhibitory genes. These antibodies recognize their antigens by binding to a specific binding site, epitope. The antibodies are either polyclonal or monoclonal antibodies. (Mäkinen & Stenbäck 2012c.)

Polyclonal antibodies are antibodies produced in living animals, usually goats, rabbits, rats or mice. They are produced by immunizing an animal with specific antigen, such as a protein or peptide. Antibodies resulting from immunization are harvested from the serum of immunized animals and then purified by affinity chromatography. When using polyclonal antibodies, the possibility of cross-reaction should be considered when interpreting the sample, since polyclonal antibodies recognize several different epitopes from the antigen that may be homologous to other proteins. (Mäkinen & Stenbäck 2012c.)

Production of monoclonal antibodies is also based on immunization of the test animal against a particular antigen. Following immunization, lymphocytes are isolated from the spleen of the test animal and then merged with cultured myeloma cells. These are selectively cultured in an immortalized hybrid cell culture, which divides endlessly and produces a single antibody molecule, a monoclonal antibody. When injected into the abdominal cavity of new experimental animal, hybridoma cells proliferate, producing a large amount of antibody that can be recovered. The advantage of monoclonal antibodies is that they are generally very specific to the antigen under study, but there may be significant differences in antibody performance between different manufacturers and between different antibody clones of the same manufacturer. (Mäkinen & Stenbäck 2012c.)

The cleaved caspase-3 (CC3) antibody is a popular marker for apoptosis of the cells (Fan & Bergmann 2010). Generally, caspases are a group of cysteine proteases. They are usually divided into two groups based on their roles in inflammation (caspases 1, 4, 5 and 12) and apoptosis (caspases 3, 6, 7, 8, and 9). Caspase-8 and caspase-9 are two major initiator caspase cascades leading to apoptosis. Caspase-3 is activated by both caspase-8 and caspase-9, and therefore is a major executioner caspase that is cleaved. Active caspase-3 disperses many cellular proteins and during apoptosis it is accountable for DNA fragmentation and morphological changes in cells. (Liu et al. 2017.) The CC3 antibody can detect big fragments of activated caspase-3, but it does not identify full length caspase-3 or other cleaved caspases (Cell Signaling Technology 2019a).

Cell growth can be determined with so-called proliferation antigens. Several of these antigens are known, but especially Ki-67 has been established for diagnostic use (Mäkinen & Stenbäck 2012a.) Ki-67 is a nuclear protein, which is expressed in many phases of the cell cycle, but not in the G0 (resting) phase (Thermo Fisher Scientific a). Ki-67 antibody indicates the number of cells in the cytokinesis; the higher the percentage, the livelier the proliferating tumor. A high degree of proliferation is associated with aggressive growth and poor prognosis in several tumors. (Mäkinen & Stenbäck 2012a.)

EGFR is a transmembrane tyrosine kinase and it belongs to the HER/ERBB protein family, which also includes Erb-B2, Erb-B3, and Erb-B4. These receptors have an important role in proliferation and tumor cell survival. (Hirsch et al. 2003.) Activation of EGFR and ERBB2 induces transphosphorylation of the ERBB dimer partner, and stimulates many different intracellular pathways, such as Ras/Raf/MEK/ERK pathway

and PI3K/Akt pathway. It has become evident that ERBB family members have a significant role in the initiation and preservation of several tumors. In both, rat and human wild-type, ERBB2 have been shown to change diploid cells. (Arteaga & Engelmann 2014.) Phospho-EGFR antibody can detect endogenous levels EGFR only when it is phosphorylated in tyrosine. There also can be cross-reaction with other activated EGFR family members, such as ERBB2. (Cell Signaling Technology 2019c.) Phospho-HER2/ERBB2 antibody only detects endogenous ERBB2 levels when phosphorylated at tyrosines 1221/1222, which are the major autophosphorylation sites in ERBB2. With this antibody, there is no cross-reaction with other activated ERBB family members or tyrosine-phosphorylated proteins. (Cell Signaling Technology 2019d.)

Extracellular signal-regulated kinases 1 and 2 (ERK1/2) belongs to a MAPK family and can mediate cell proliferation and apoptosis. Protein kinases are key components of the cell signaling network and they can be activated from extracellular stimuli, such as growth factors, hormones or heat stress. Phosphorylation of MEK leads to the phosphorylation of ERK1/2, on both threonine and tyrosine. Phosphorylated ERK phosphorylates ribosomal s6 kinase (RSK) and translocate to the nucleus. Together ERK and RSK activate many transcription factors leading to protein synthesis and producing alterations in cell proliferation and survival. (Mebratu & Tesfaigi 2009.) Phospho-p44/42 MAPK (ERK1/2) antibody can detect endogenous levels of ERK1 (p44) and ERK2 (p42) MAPK when either only phosphorylated at threonine 202 or phosphorylated at both threonine 202 and tyrosine 204 (Cell Signaling Technology 2019e).

Akt is also known as protein kinase B (PKB). It has an important role in many cellular functions, i.e. transcription, metabolism, proliferation, growth and survival. (Hers, Vincent & Tavaré 2011.) Amongst other factors, variety of growth factors and for example insulin can activate the Akt signaling cascade, which activates other factors, such as PI3K, and ultimately leads to the phosphorylation of Akt. Akt is fully activated when it is phosphorylated on both sides, the activation loop (threonine 308) and hydrophobic motif (serine 473). After activation Akt detaches from the membrane and phosphorylates various substrates in the nucleus and cytoplasm, thus influencing on different cellular events. (Kanan et al. 2010.) Dysregulation of Akt can lead to various illnesses, for example cancer or diabetes (Hers et al. 2011). Phospho-AKT rabbit antibody can detect endogenous levels of Akt only when it is phosphorylated at serine 473 (Cell Signaling Technology 2019b).

4.3.5 Counterstaining

Counterstaining is done after immunohistochemical stains. It is used to enhance the tissue morphology and contrast. Most commonly counterstaining is done with hematoxylin, which binds to nuclei resulting purplish-blue stain. In counterstaining the exposure to the hematoxylin is brief, from 30 seconds to 1 minute, and the tissue slide is rinsed with distilled water after staining. (Jiang & McKeegan 2015: 81-82.)

4.4 Dehydration, mounting and slide coating

After staining protocol, the tissue slides are dehydrated again before adding a coverslip. Dehydration is done through alcohol series with increasing ethanol concentrations and rinsed in xylene several times. (Jiang & McKeegan 2015: 81-82.) When mounting and cover slipping the slides it is important to maintain the transparency to stained tissue sections. This is particularly important when imaging slides. Mounting media should be suitable for used stains. Most histopathology laboratories use non-aqueous mounting media. When mounting the slides, appropriate amount of mountant is added on the slide and a coverslip, which coats the tissue section surface, is placed on it. The air bubbles must be removed under the coverslip. (Moon 2013: 601.)

5 The Verschuren group

The Verschuren group has a comprehensive approach to lung cancer research. They are studying the lung cancer drivers biological properties in their physiological complex microenvironment. This knowledge is combined to building diagnostic models of lung cancer. The main goal of the Verschuren group's research is to collect more information about lung cancer and study new strategies for prevention, and intervention in progression of lung cancer. They have progressed in lung cancer research from murine lung cancer cohorts to human lung cancer cohorts. (FIMM 2019.)

The Verschuren group has existing collaboration with oncologist and surgeon from Cardiovascular and thoracic surgery clinic, Helsinki University Central Hospital, and pathologists from Department of Pathology/HUSLAB, University of Helsinki. They collect mainly NSCLC samples and patient-matched healthy lung tissue. The samples are

freshly brought to the laboratory. They also get formalin-fixed paraffin-embedded (FFPE) tumor blocks from Department of Pathology, which are used to histology-spesific tissue microarrays of AC, SCC, and adenosquamous carcinoma (ASC) histotypes. They are used to validate clinical NSCLC findings. (Talwelkar 2019.)

We are very happy we got to work with this research group as their work is very interesting and meaningful. The project team consists of 6 group members: Emmy Verschuren (FIMM-EMBL Group Leader), Jie Bao (FIMM-EMBL Doctoral Student), Iris Lähdeniemi (Post-doctoral Researcher), Ashwini Nagaraj (Doctoral student), Nora Linnavirta (Laboratory Technician), and Sarang Talwelkar (FIMM-EMBL Doctoral Student). (FIMM 2019.)

6 The purpose, aim and research questions

The Verschuren group's long-term aim is to examine new strategies for intervening and preventing lung cancer progression. We were just alongside for a short period of time, so the main purpose of our thesis project was to analyze the results of driver gene targeted drugs on murine and human lung cancer tissue. Our aim was to analyze the results and collected data from the samples. We used methods developed by the research group. The Verschuren group will receive the analyzed results and reports of the thesis, and they may use them for their own purposes in the future.

The research questions leading this thesis project:

1. How the selected drugs effect on the treated tissue samples?
2. Is combination drug treatment more effective compared to single drug treatment?
3. Does drug treatment have similar effects on murine and human tissue samples?

7 Workflow

In our thesis project we worked with surgically resected lung tumor tissues from Genetically engineered mouse models (GEMMs) and human cancer patients. The Verschuren group have developed their own tissue slice technology. They have

published a video and an article about the method in November 2018 in Journal of visualized experiments (JoVE) (Nagaraj et al. 2018). We used that method to process and treat samples *ex vivo* with AF and TR or their combination. *Ex vivo* means biological activity performed outside a living organism, but still within a living cell, tissue or biological macromolecule. The used drugs were specifically selected by the Verschuren group, based on previous studies and their previous experiences. After the drug treatment we compared treated tissues to control tissues (0 h and DMSO treated) to evaluate the drug response. Machine learning was done only for the murine samples. Morphology of the human samples differed from each other and time was very limited, therefore we decided only to demonstrate the machine learning for the murine samples. The workflow with tissues is described later on (figure 5).

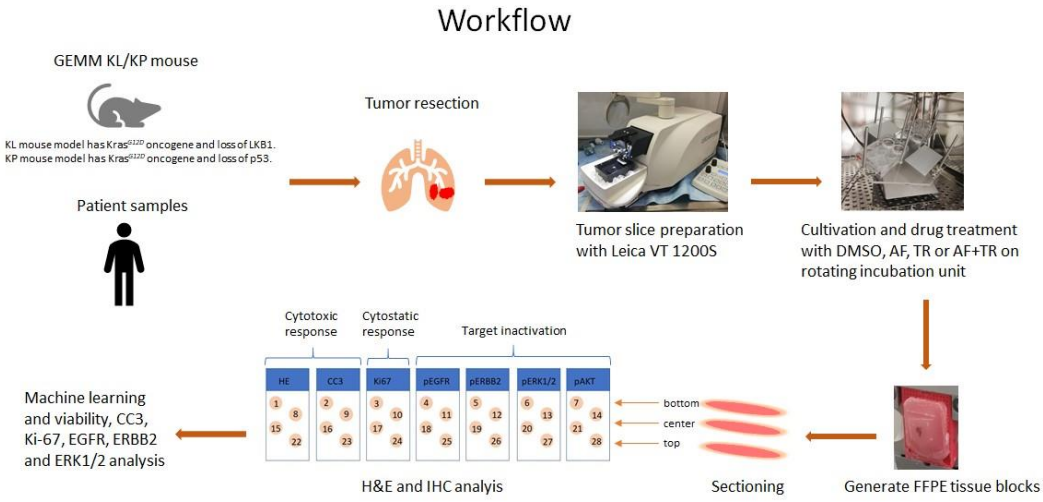

Figure 5. Workflow (Nagaraj et al. 2018).

7.1 Murine samples

We used two GEMMs of NSCLC. KL mouse model has *Kras*^{G12D} oncogene and loss of *Lkb1*. KP mouse model has *Kras*^{G12D} oncogene and loss of *p53*. Mice were infected intranasally by using adenoviruses either Ad5-SPC-Cre or Ad5-CC10-Cre. Those mainly target Cre recombinase to alveolar type II cells (SPC) or to bronchiolar club cells which express club cell antigen 10 (CC10). KP mice will develop AC tumors and KL mice will develop AC or ASC tumors after the infection. (Närhi et al. 2018; Nagaraj et al. 2017.)

Mice were sacrificed by following the ethical guidelines and tumors were resected from normal lung tissue.

We had four GEMM samples: Sample 181017 was ASC tumor bearing KL mouse, infected with Ad5-CC10-Cre, where treatment was done 24 hours with DMSO, TR, AF, and TR+AF with different concentrations. Sample 050618 was also ASC tumor bearing KL mouse, infected with Ad5-CC10-Cre. With this sample we had two tumor samples T1 (tumor 1) and T2 (tumor 2), where on both, the treatment was done 24 and 72 hours with DMSO, TR, AF, and TR+AF. Sample 311017 was AC tumor bearing KP mouse, infected with Ad5-SPC-Cre, where treatment was done 24 hours with DMSO, TR, AF, and TR+AF with different concentrations.

7.2 Human samples

Lung AC, SCC or ASC tumors were surgically resected from cancer patients and samples were freshly brought to the laboratory. We had three human samples: Sample PLT76 was lung SCC, molecular alterations not known. Treatment was done for 24 hours with DMSO, TR, AF and TR+AF. Slicing was performed inside chemical hood, but it did not go well as the tissue was too soft. White cottony tissue was disturbing the slicing. Sample PLT73 was lung AC with *EGFR Ala767_Val768dub* mutation. Treatment was done for 24 hours with DMSO, AF, and TR+AF, and for 72 hours with DMSO, TR, AF, and TR+AF. Slicing was performed inside chemical hood. Tissue was of intermediate stiffness, not too soft. Slicing went well for first 6 slices, after which tissue was spongy and whitish cotton like structures started to come off. After this the tissue was not sliceable. Left over tissue after slicing was fixed. Sample PLT82 was lung AC, molecular alterations not known. Treatment was done for 24 and 72 hours, both with DMSO, TR, AF, and TR+AF. Slicing went well for first 7 slices, after that the tissue started to break down.

7.3 Sample processing

Media and drugs (AF, TR and their combination) were prepared, drugs were diluted in DMSO, which also worked as a control to evaluate the effects of culturing, for example the number of dead cells after 24-hour treatment. Tissue preparation was started by slicing tumor tissue to 200 µm thick slices using Leica VT 1200S machine (figure 6). During the slicing samples were kept on ice in Hanks Balanced Salt Solution (HBSS).

Slices were placed to a grid in a six well plate with media and drugs. Depending on the amount of tumor slices, slices were treated for 24 to 72 hours in a rotating incubation unit (+37 ºC). If there were not enough slices the treatment was only done for 24 hours. 0 h control samples were fixed with 10 % neutral buffer formalin overnight at 4 ºC after slicing.

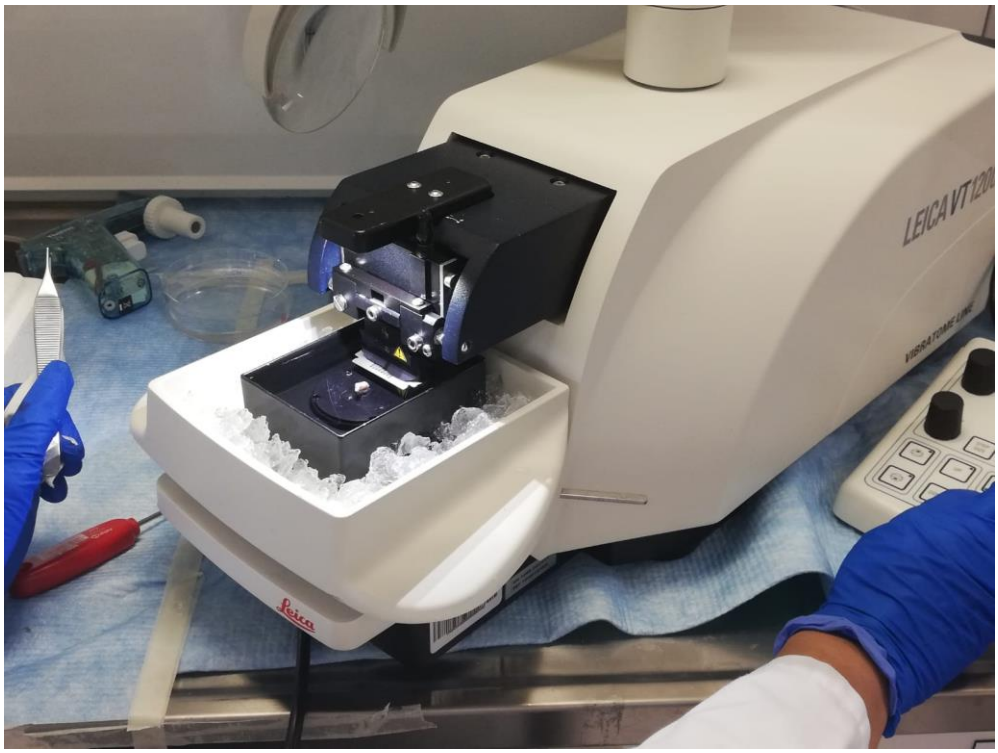

Figure 6. Leica VT 1200S.

Tissue slices were fixed with 10 % neutral buffer formalin overnight at 4 ºC at the end of the treatment. After this, tissue slices were processed into paraffin-embedded blocks using a microwave processing machine (KOS, MILESTONE). Embedding was done by placing the grid side of the tumor up because mostly the air side is more viable, and then trimming would not harm the most representative side of the tumor. By using microtome FFPE tissue blocks were sectioned to 4 µm thick sections. On total there were seven slides per sample and sectioning was done by sectioning first one section to all slides before starting a next round to have a comprehensive view of tumor slices. First sections are from the grid side of the tumor slice, middle sections represent the middle part of the tumor slice, and last sections represent the air side of the tumor slice. Usually the air side is more viable than the grid side. Slides were stained using H&E, and a chromogenic IHC using different primary antibodies (pERBB2, CC3, Ki-67, pAKT, pERK1/2, and

pEGFR for some experiments), and HRP-DAB for visualization of the staining (figure 7). Antigen retrieval was done with Tris EDTA pH 9.0 or citric acid pH 6.0.

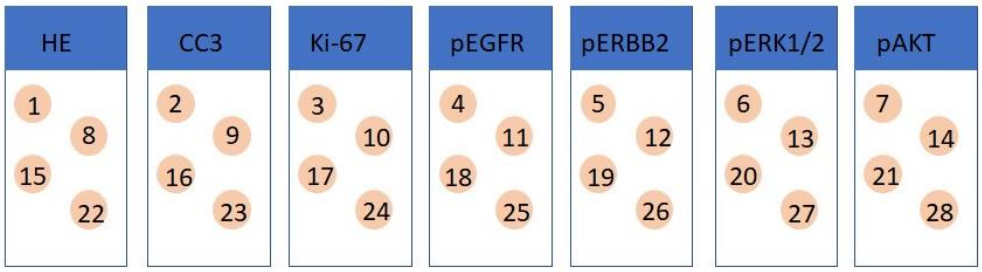

Figure 7. Sectioning and staining plan for slides.

7.4 Imaging and image analysis by machine learning

The stained tissue sections were scanned with a Pannoramic slide scanner. Scanned pictures were processed with Pannoramic Viewer. The most viable and representative tissue sections were selected from H&E stained slides. From IHC stained slides, a tissue section closest to selected H&E stained tissue was selected. For example, if the selected H&E stained tissue was fourth section on the slide, then also fourth section from IHC stained slides were chosen. In some cases, the same tissue section was not representative, then the most representative tissue section was selected. Original scanned pictures were huge, therefore pictures needed to be downsized for further analysis. H&E stained tissue images were exported from original scans in a 1:4 ratio, and they were subsequently processed to acquired a tiff format using ImageJ software. Snapshots with same magnification per experiment were taken from H&E and IHC stained tissue sections to quantify the molecular pathway alteration on tissues. To evaluate drug response, the drug treated tissues were compared to control tissues, closest 0 h and DMSO treated tissue.

CL2M software was used to machine learning. At first images were segmented using a superpixel-based algorithm, where the software groups the similar areas together, based on the picture texture and intensity. (Ren & Malik 2003.) Then we created classes in the software, which will separate the segmented regions into either ‘Viable cell’, ‘Dead cell’,

‘Stromal and other cell’, or ‘Artifact and background’ categories. During machine learning process, a training session was firstly performed, where representative regions for each class were selected manually, and the software learned from the features to predict the whole image by itself. This analysis was done image by image, because samples were pathologically so different, and experimental conditions differed from each other (slicing, culturing, drug treatment) which might have affected on cell morphology. For machine learning multiple rounds needed to be done, to correct some wrongly recognized cells. One example of difficult case for analysis is to distinguish between stromal cells and necrotic tumor cells in tissues post cultivation or drug treatment. The software was trained to recognize necrotic cells from viable cells based on the nuclei morphology: cells with i.e. pyknotic or fragmented nucleus were marked as a dead cell. But after cultivation and drug treatment, stromal cells also die and look similar to necrotic tumor cells (figure 8). Machine learning result will never be 100 % correct, but it can give a good overview of tissue viability. These results were compared to H&E and IHC staining’s (can be judged by bare eyes) to find out if the results were consistent. All pictures were gathered up on PowerPoint to make the final conclusions.

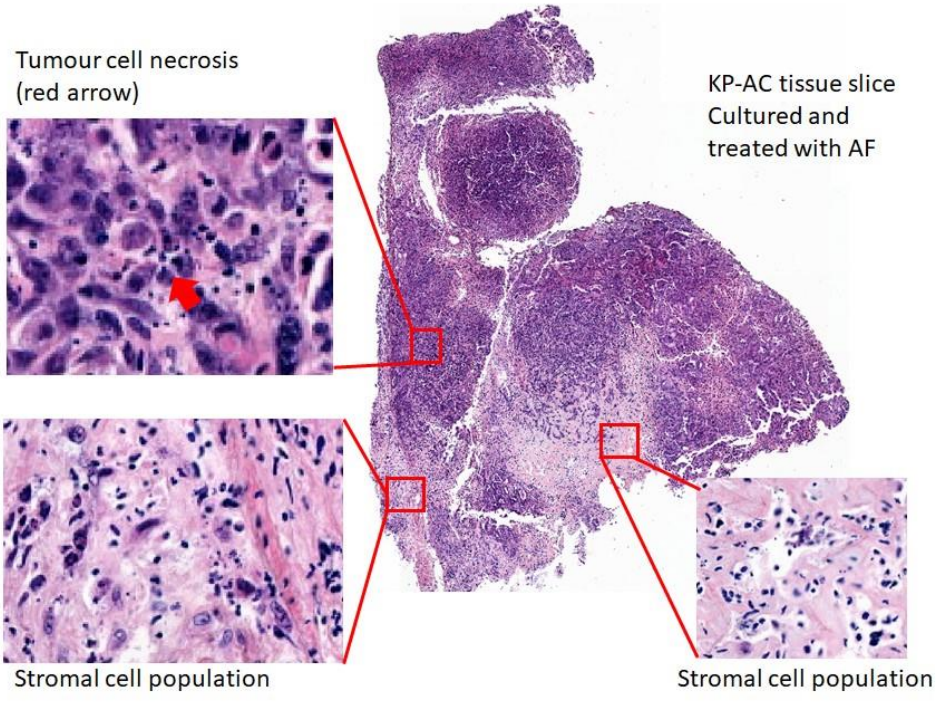

Figure 8. Stromal cells, particularly unhealthy/dead stromal cells can interfere with necrosis machine-learning (Bao 2019).

8 Results

On total, we had seven samples suitable for processing and analyzing. Four of them were murine lung cancer tumor samples and three of them human lung cancer tumor samples. Three of the murine samples were ASC and one AC. Two of the human samples were AC and one SCC. The samples showed no significant difference in H&E viability analysis, apart from one ASC murine sample (181017) which showed cytotoxic response upon combination treatment. In CC3 analysis, two human AC samples showed modest increase in cytotoxicity, and only one of the ASC sample had increased cytotoxic response. In Ki-67 analysis, one AC and one ASC murine sample showed decreased cytostatic response following combination treatment. Quantification of CC3 and Ki-67 positivity is still required for further conclusion. Target inactivation analysis was done with EGFR, ERBB2 and ERK1/2. Following AF treatment, EGFR and ERBB2 activity was not completely inhibited, but it was decreased in almost every sample. ERK1/2 activity was effectively blocked or reduced in all the samples following TR treatment. With human samples, quantification of the viable cells was challenging due to lot of stroma and matrix components (table 1).

Table 1. Result summary.

		H&E	CC3	Ki-67	pEGFR	pERBB2	pERK1/2
Murine	181017 (KL;ASC)	Cytotoxic response upon combination treatment	Increased following single and combination treatment	Decreased following combination treatment	Not completely inhibited following 24 h AF treatment	Not completely inhibited following 24 h AF treatment	Effectively blocked upon 24 h TR treatment
	311017 (KP;AC)	No significant difference* (stromal cells interfere)	No significant increase**	Decreased following combination treatment	-	Reduced during 10 µM AF treatment	Effectively blocked upon 24 h TR treatment
	050618: T1 (KL;ASC)	No significant difference*	No significant increase**	No significant difference**	-	Incomplete inactivation during 72 h AF treatment	Reduced during 24 h TR treatment
	050618: T2 (KL;ASC)	No significant difference*	No significant increase**	No significant decrease**	-	Incomplete inactivation during 72 h AF treatment	Reduced during 24 h and 72 h TR treatment
Human	PLT73 (AC)	No significant difference* (stromal cells)	Modest increase** (72 h)	No significant difference*	Decreased during AF treatment	Decreased during AF treatment	Decreased**
	PLT76 (SCC)	No significant difference*	No significant increase**	No significant decrease**	Low EGFR activity at 0 h	Reduced**	Reduced/loss of activity in DMSO
	PLT82 (AC)	No significant difference* (stromal cells)	Modest increase** (72 h)	No decrease**	-	Reduced in 72 h DMSO	Reduced/ Absent in 72 h DMSO

*between controls and treated samples **following single or combination treatment

8.1 Drug response analysis of murine samples

Sample 181017 was ASC tumor from KL mouse, treatment was done for 24 hours with single and combination drugs, and different AF concentrations. Viability analysis of H&E staining showed most cytotoxic response upon combination treatment (figure 9). Machine learning based necrosis quantification done with CL2M software presented consistent results (figure 10 and 11). TR+AF5 treated tissue had more dead cells compared to controls (0h B and DMSO B). Cytotoxic response was analyzed with CC3. There appeared to be increased CC3 positivity following single agents as well as combinatorial treatment (figure 12). Cytostatic response was analyzed with Ki-67. Positivity of Ki-67 appeared to be decreased following combinatorial drug treatment (figure 13). Target inactivation was measured with pEGFR, pERBB2, and pERK1/2. EGFR was not completely inhibited following AF treatment, compared to lower concentrations 10 µM appeared to be more effective in inhibiting EGFR activity (figure 14). ERBB2 was not completely inhibited following AF treatment (figure 15). ERK1/2 activity was effectively blocked upon TR treatment (figure 16). Quantification of CC3 positive areas and Ki-67 positive nuclei is still required for further conclusion. With ERBB2 longer time points may need to be tested.

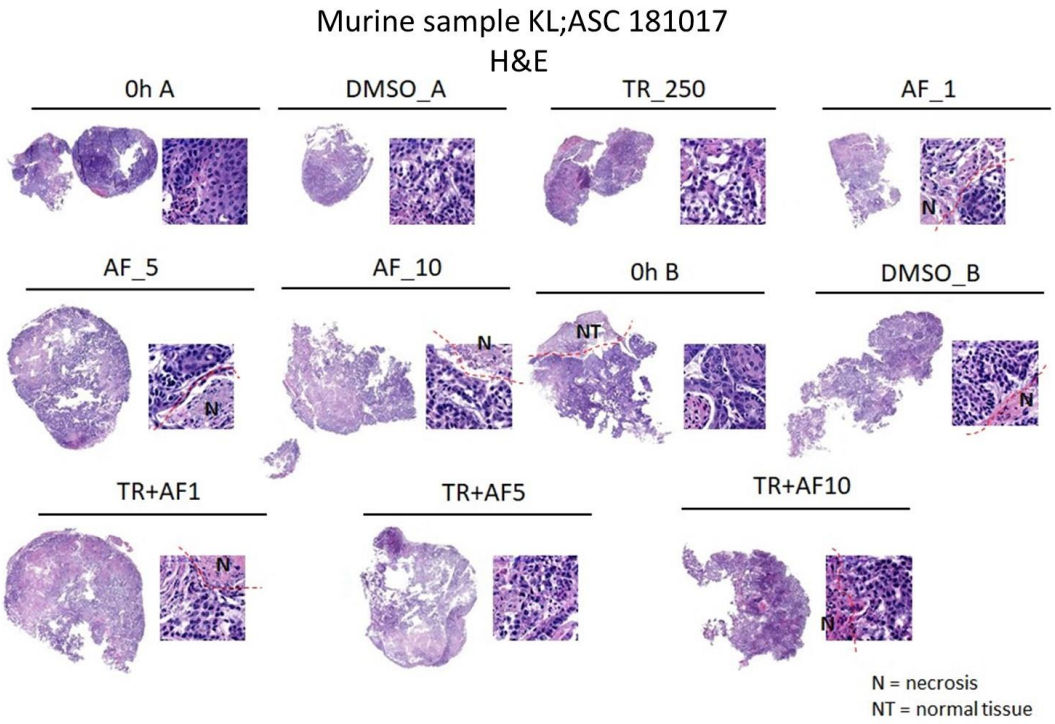

Figure 9. Viability analysis for the H&E stained tissue sections. There appears to be cytotoxic response upon combination treatment.

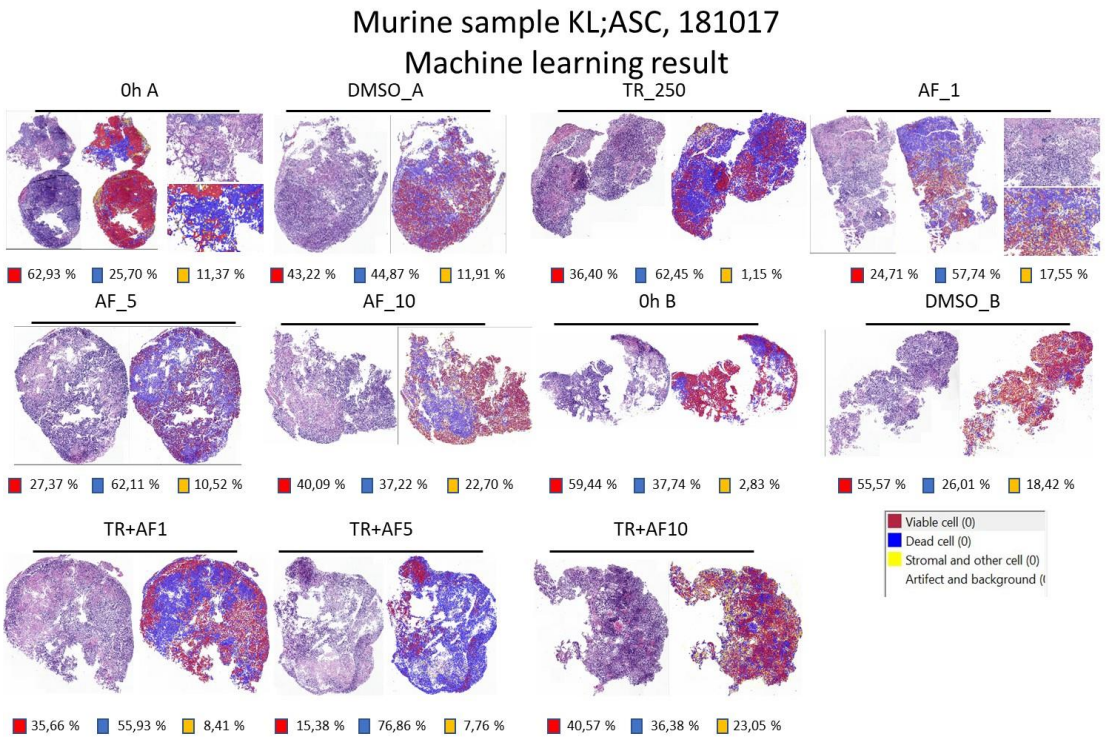

Figure 10. Machine learning based necrosis quantification with CL2M software.

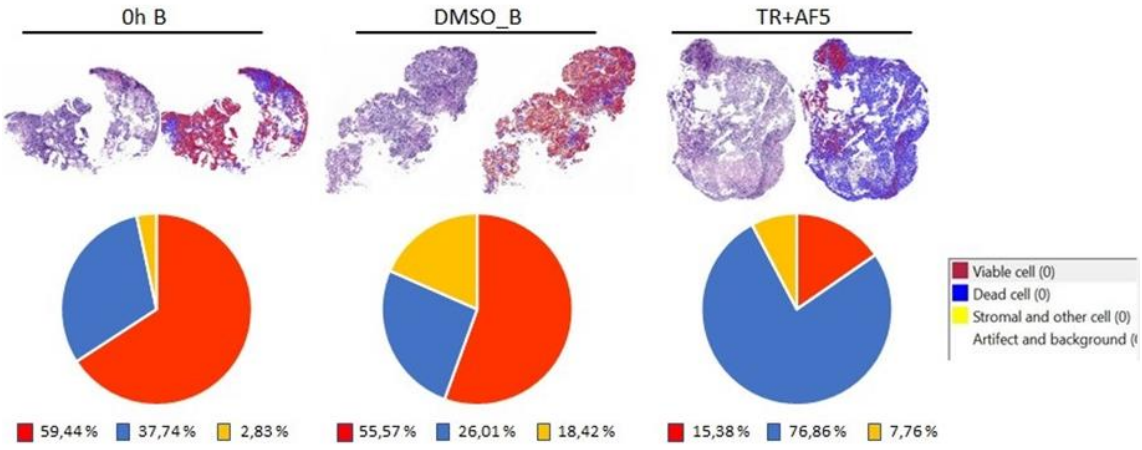

Figure 11. Machine learning result from murine sample KL;ASC 181017 shows increased cytotoxicity after combination treatment.

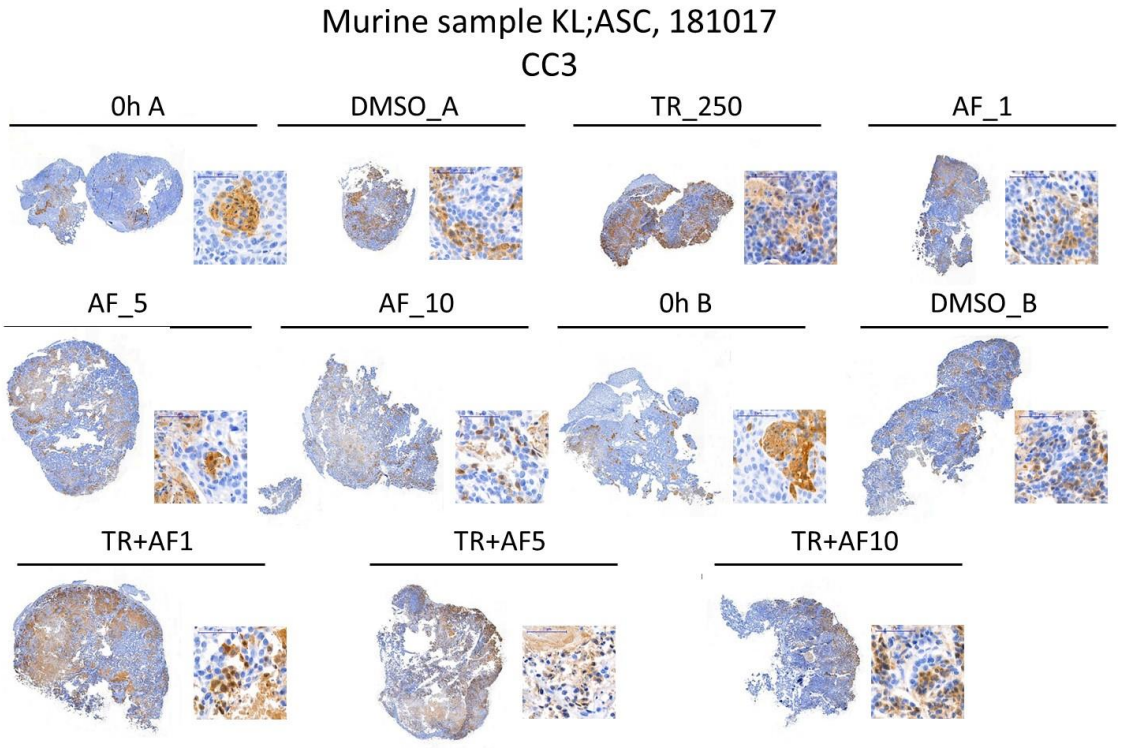

Figure 12. Analysis of cytotoxic response.

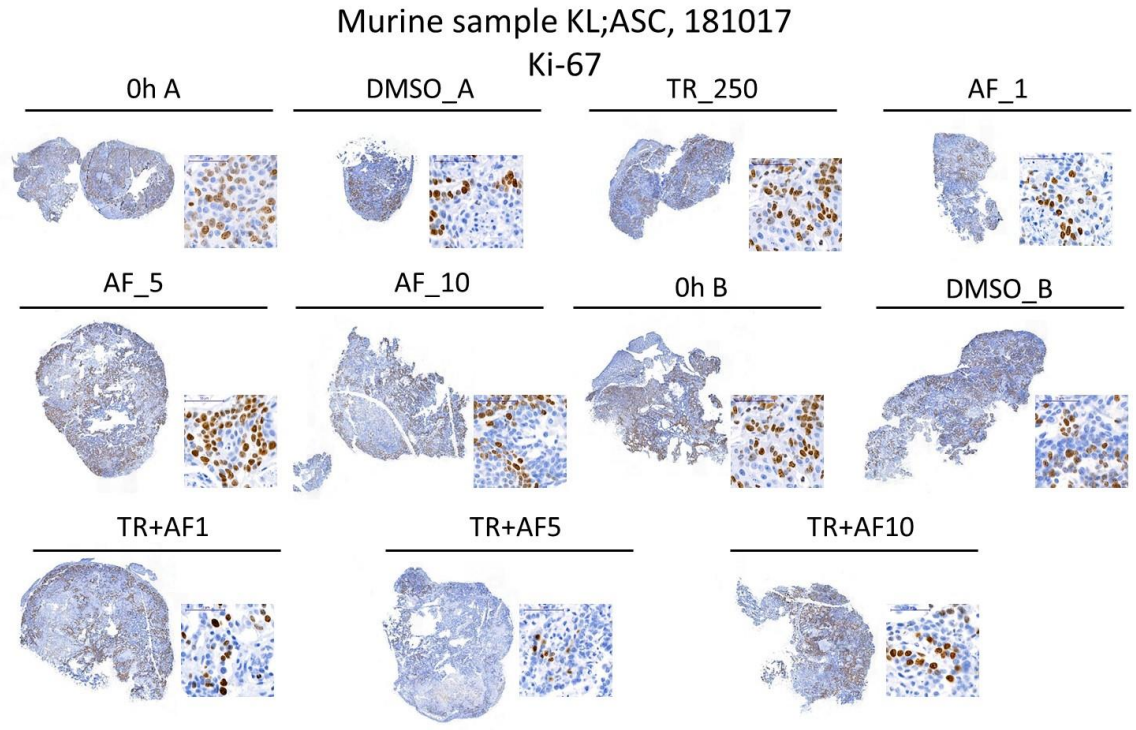

Figure 13. Analysis of cytostatic response.

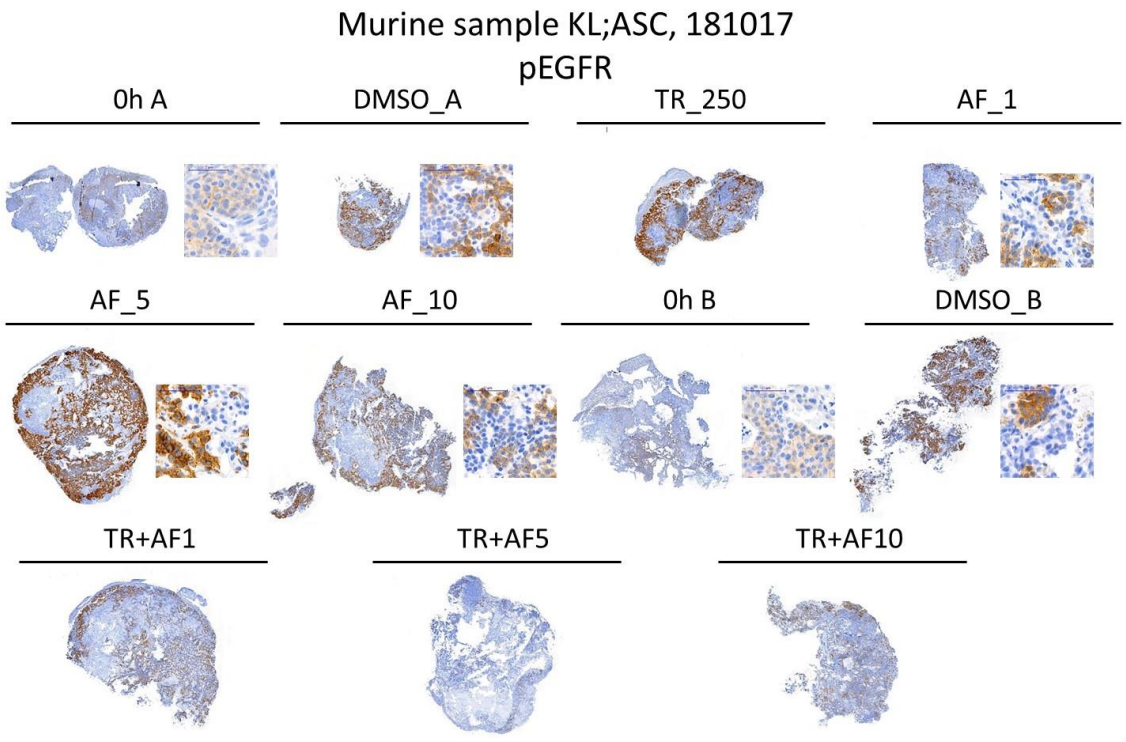

Figure 14. pEGFR analysis of target inactivation following AF treatment.

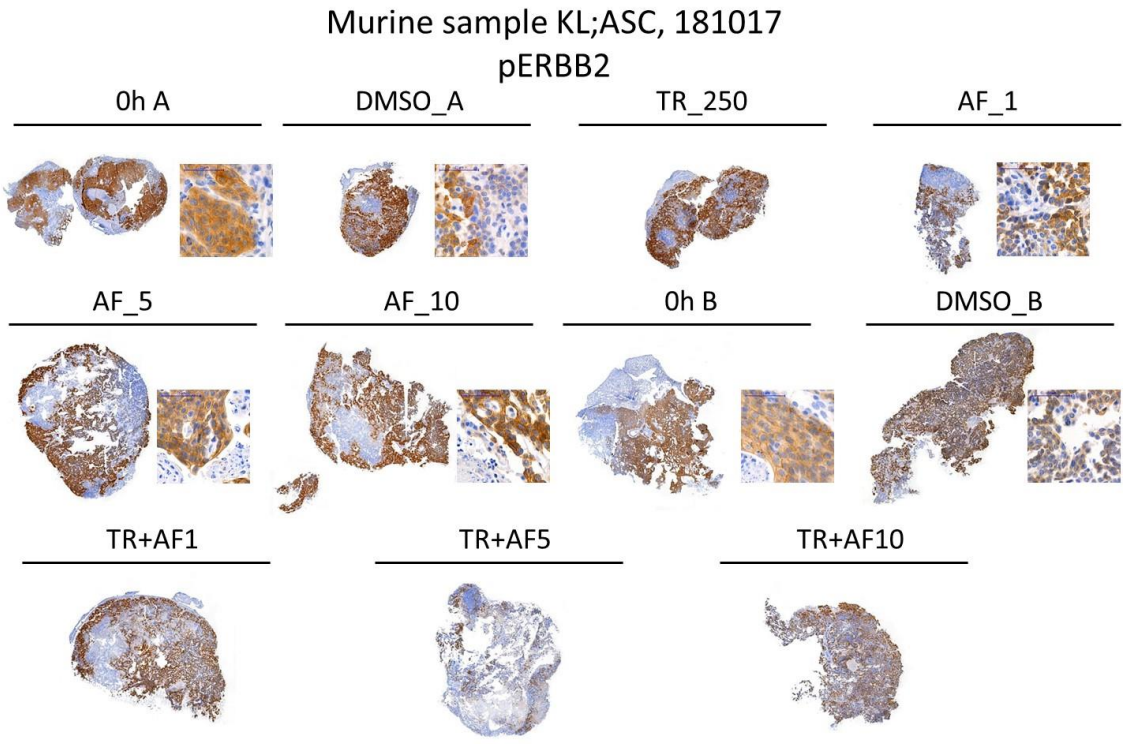

Figure 15. pERBB2 analysis of target inactivation following AF treatment.

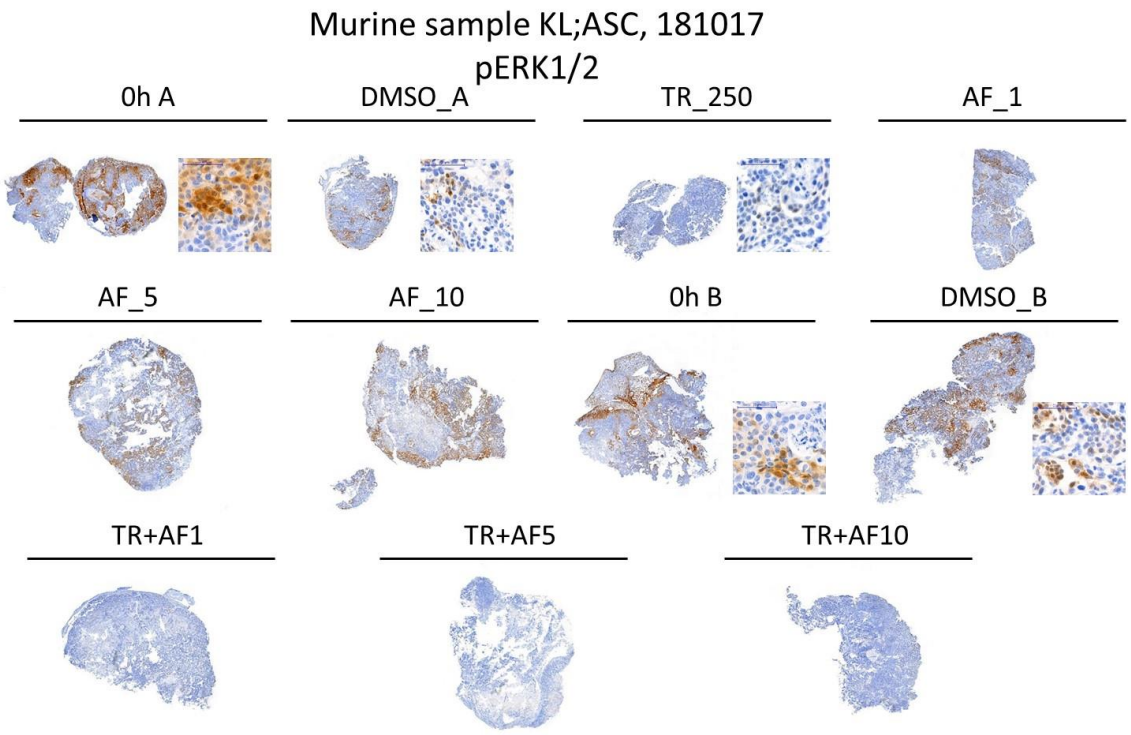

Figure 16. pERK1/2 analysis of target inactivation following TR treatment.

Sample 050618 was also ASC tumor from KL mouse, with this sample we had two tumor samples T1 and T2, treatment was done for 24 and 72 hours with single and combination drugs. T1 viability analysis of H&E staining and machine learning necrosis quantification did not show significant difference between controls and drug treated tissues. Cytotoxicity analysis did not show any significant increase in CC3 positivity during drug treatments when compared to DMSO. Cytostatic analysis done with Ki-67 showed no significant difference in the Ki-67 positive nuclei between the treated samples and DMSO. Target inactivation was measured with pERBB2 and pERK1/2. There was incomplete inactivation of ERBB2 during 72 h AF treatment and increased ERBB2 activity following TR treatment. Low baseline ERBB2 activity in 0 h samples appear to correlate with lack of treatment response. pERK1/2 activity is reduced during 24 h TR treatment when compared to DMSO. However, upon 72 h TR treatment pERK1/2 activity is not significantly different compared to DMSO, which might be due to resistance to TR treatment. The gathered images of this sample can be found in the appendix 1.

The T2 sample of 050618 viability analysis of H&E staining and machine learning necrosis quantification did not show significant difference between DMSO and drug treated tissues, 0 h controls appear to be more viable than cultured tissues. Compared

to DMSO, cytotoxic CC3 analysis did not show significant increase in CC3 positivity during drug treatments. Ki-67 analysis of cytostatic response did not show significant decrease in Ki-67 positivity during drug treatments when compared to DMSO. Target inactivation was measured with pERBB2 and pERK1/2. There was incomplete inactivation of ERBB2 during 72 h AF treatment and increased ERBB2 activity following 24 h culture (DMSO). Low baseline ERBB2 activity in 0 h samples might be related with poor treatment response. pERK1/2 activity was reduced following 24 h and 72 h TR treatment. The gathered images of this sample can be found in the appendix 2.

Sample 311017 was AC tumor from KP mouse, treatment was done for 24 hours with single and combination drugs, and different AF concentrations. This sample had a lot of stromal cells, which affected the machine learning and the results were not consistent (figure 17). Cytotoxic response was analyzed with CC3, which showed no significant difference following single or combinatorial drug treatment. Cytostatic analysis was done with Ki-67, which appears to show decreased Ki-67 positivity in TR+AF treated samples, when compared to DMSO. Quantification for CC3 and Ki-67 needs still to be done to make further conclusions. Target inactivation was analyzed with pERBB2 and pERK1/2. With pERBB2, 10 µM AF was most effective in reducing ERBB2 activity. pERK1/2 activity was effectively blocked upon 24 h TR treatment. The gathered images of this sample can be found in the appendix 3.

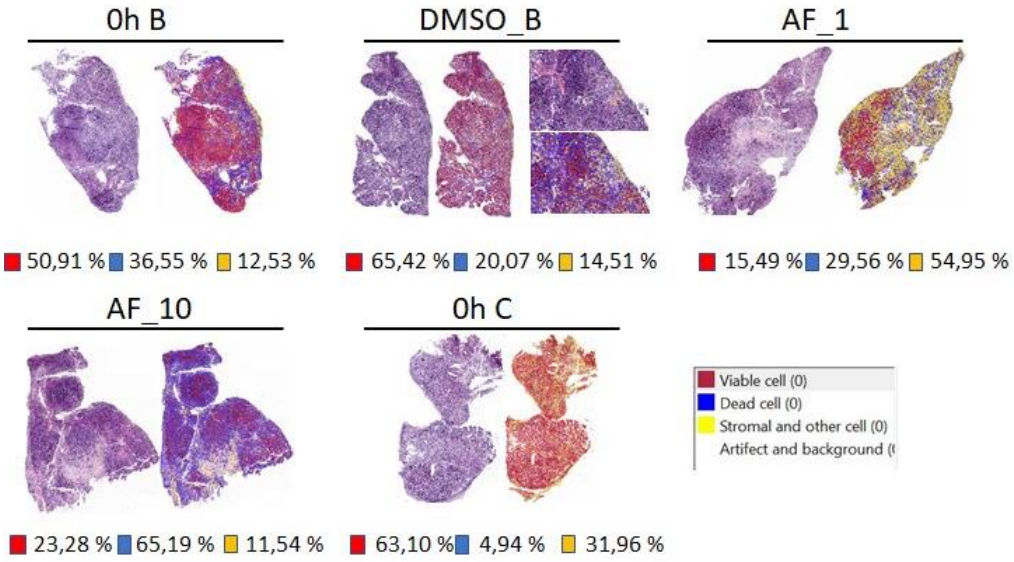

Figure 17. Machine learning result from sample KP;AC 311017. The number of stromal cells in the tissue slices differed which make machine learning problematic, as even 0 h controls had a different number of stromal cells.

As a conclusion, we had three KL;ASCs, and one KP;AC-derived tissue slices were treated with TR, AF, or TR+AF for 24 h or 72 h and then analyzed. All the machine learning results are gathered to the figure 18. Only one of the three KL;ASC-derived tissue slices appeared to have increased cytotoxic response (necrosis and CC3 positivity) upon single and combinatorial TR+AF treatment. Quantification of CC3 and Ki-67 positivity is still required for further conclusion. Lack of treatment responses in two of the three KL;ASC-derived tissue slices could possibly be due to low baseline ERBB2 activity. Tissue slices showed incomplete inactivation of ERBB2 receptors following 24 h and 72 h AF treatment. There also appeared to be hyperactivation of ERBB2 receptors in ASC slices following TR treatment.

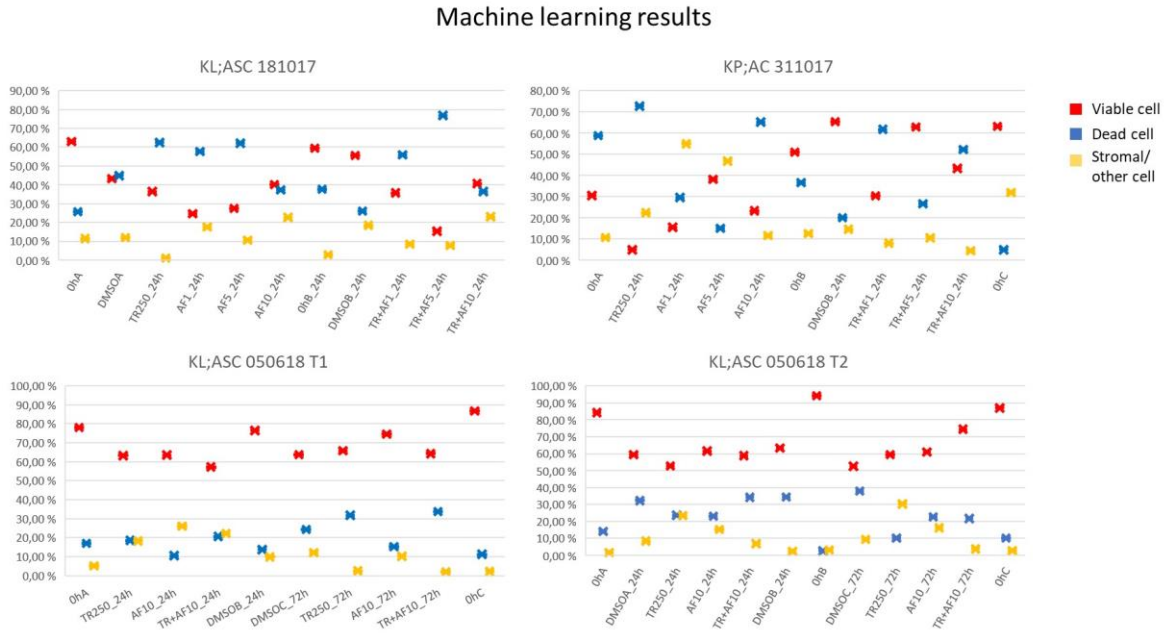

Figure 18. Machine learning result summary from GEMM lung cancer samples.

8.2 Drug response analysis of human samples

Sample PLT76 was lung SCC molecular alterations were not known, treatment was done for 24 hours with DMSO, TR, AF and TR+AF. Viability analysis of H&E stained tissue sections shows no significant difference in the viability of the drug treated compared to DMSO treated samples. Cytotoxicity analysis did not show any significant increase in CC3 positivity during drug treatments when compared to DMSO. Ki-67 analysis of

cytostatic response shows no significant decrease in Ki-67 positivity upon drug treatment when compared to DMSO. Target inactivation was analyzed with pEGFR, pERBB2 and pERK1/2. There was low EGFR activity at treatment onset, in 0 h control, and reduced EGFR activity in the DMSO-treated sample. pERBB2 activity was reduced in AF and AF+TR treated samples compared to DMSO and pERK1/2 activity was reduced in DMSO-treated sample compared to 0 h control. The gathered images of this sample can be found in the appendix 4.

Sample PLT73 was lung AC with *EGFR Ala767_Val768dub* mutation, treatment was done for 24 hours with DMSO, AF, and TR+AF, and for 72 hours with DMSO, TR, AF, and TR+AF. Viability analysis of H&E stained tissue sections shows no significant difference in the viability of the drug treated compared to DMSO treated samples, although sample have a lot of stroma cellular matrix component compared to epithelial cells. Cytotoxicity analysis shows modest increase in CC3 positivity upon 72 h single or combinatorial drug treatment when compared to DMSO. For further conclusions quantification needs to be done. Cytostatic analysis shows no significant difference in Ki-67 positivity between drug treated compared to DMSO treated samples. Target inactivation was analyzed with pEGFR, pERBB2 and pERK1/2. There appear to be hyperactivation of EGFR and ERBB2 in DMSO treated sample compared to 0 h. Also compared to DMSO, pEGFR and pERBB2 positivity appears to be decreased following 24 h and 72 h AF treatment. pERK1/2 positivity appears to be decreased following 24 h and 72 h AF or TR treatment compared to DMSO. The gathered images of this sample can be found in the appendix 5.

Sample PLT82 was lung AC, molecular alterations not known, treatment was done for 24 and 72 hours, both with DMSO, TR, AF, and TR+AF. Sample had lot of stroma and matrix component compared to epithelial cells and it was morphologically very different looking AC. Overall, there was no significant difference in the gross morphology and cellular features between drug-treated and DMSO-treated samples (figure 19). Further evaluation with the pathologist is required to make final conclusions. Cytotoxicity analysis shows modest increase in CC3 positivity upon 72 h single and combinatorial drug treatment (figure 20). Cytostatic analysis shows no decrease in Ki-67 positivity upon single and combinatorial drug treatment compared to DMSO (figure 21). Target inactivation was analyzed with pERBB2 and pERK1/2. ERBB2 activity was reduced in 72 h DMSO-treated sample compared to neighbouring 0 h sample (figure 22). Reduced

or absence of pERK1/2 activity in 72 h DMSO-treated sample compared to neighbouring 0 h sample (figure 23).

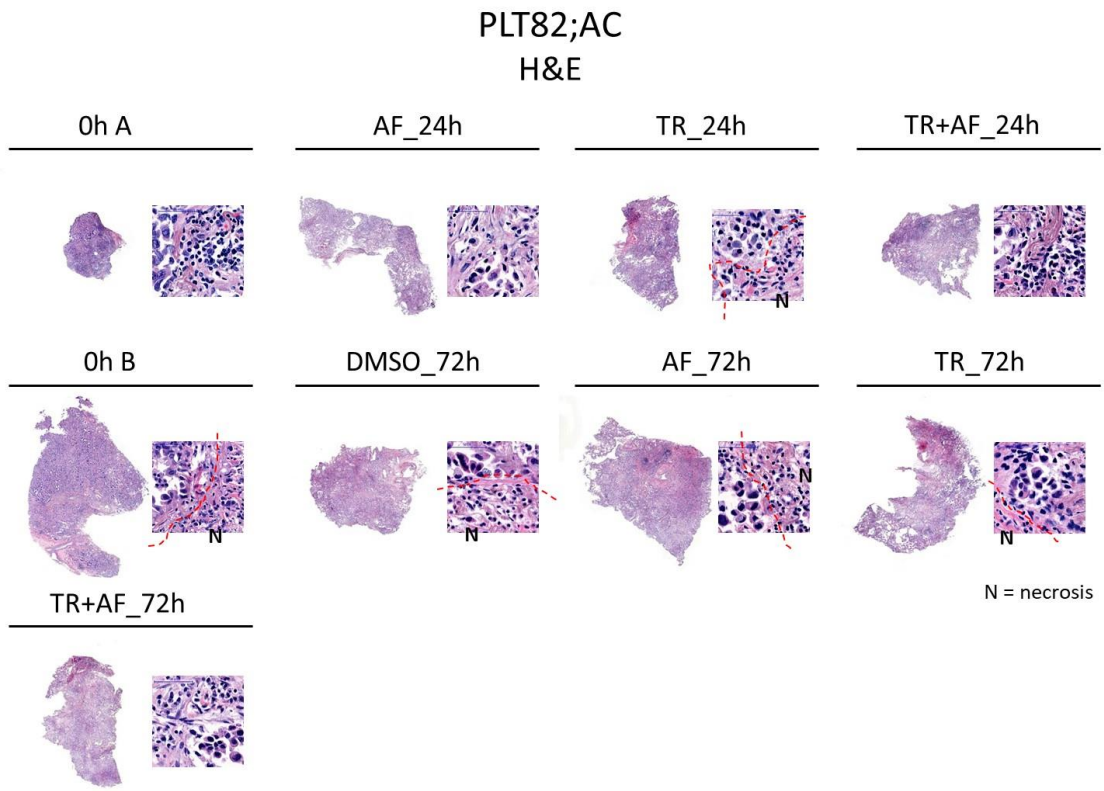

Figure 19. Viability analysis for the H&E stained tissue sections. Morphologically very different looking AC: A lot of stroma and matrix component.

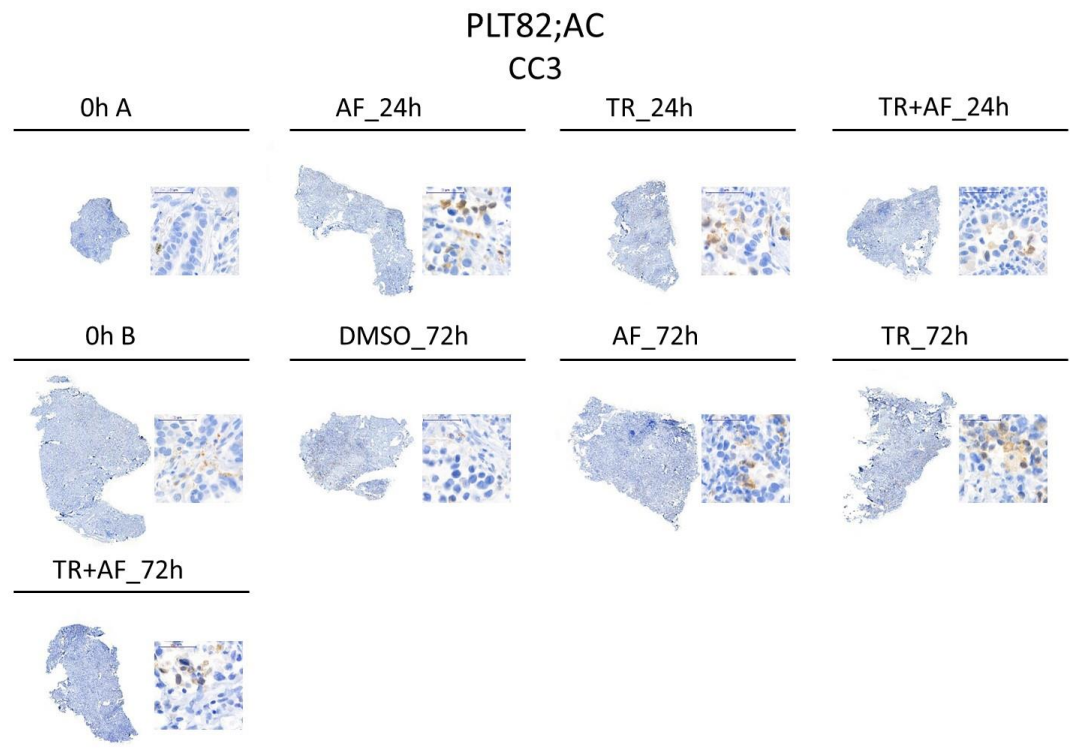

Figure 20. Analysis of cytotoxic response.

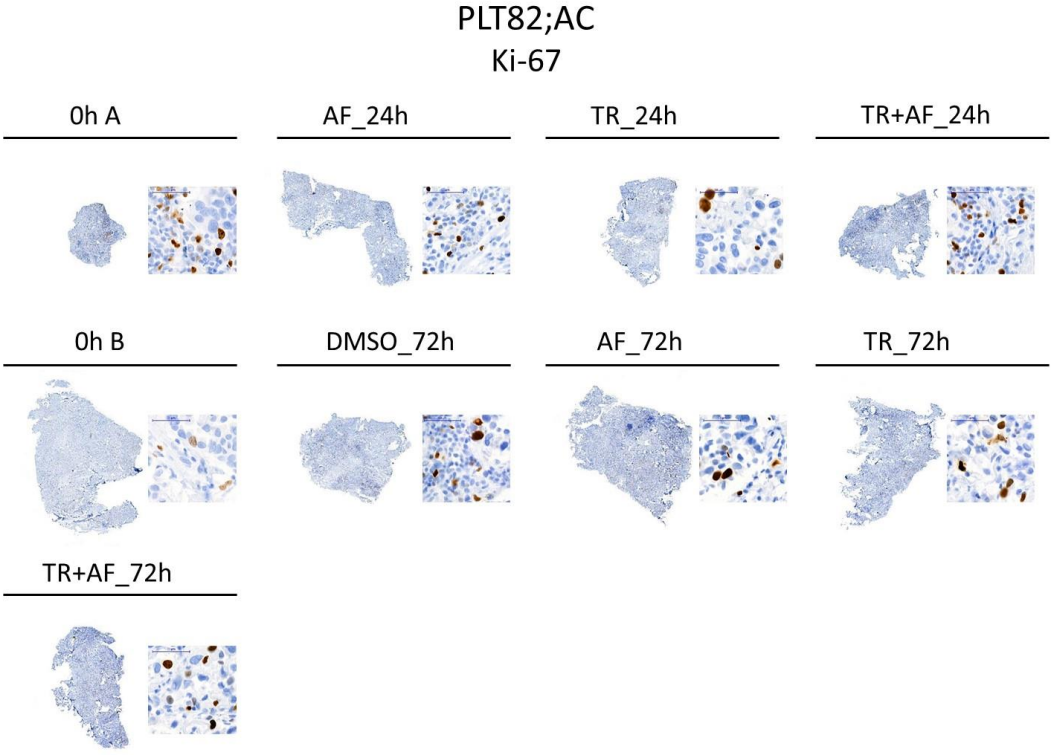

Figure 21. Analysis of cytostatic response.

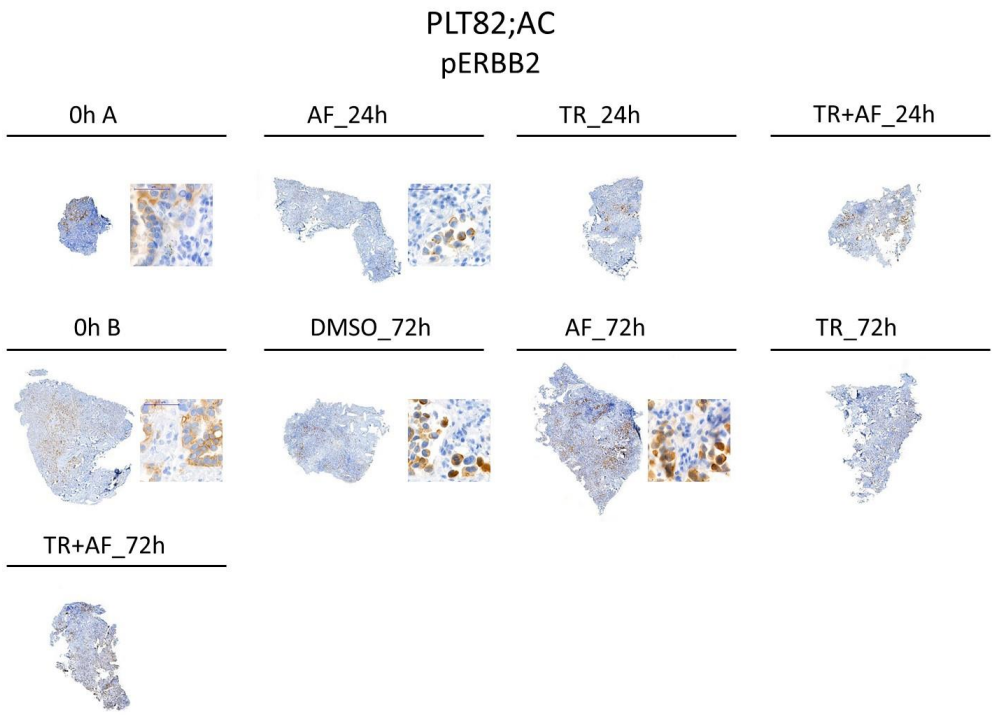

Figure 22. pERBB2 analysis of target inactivation following AF treatment.

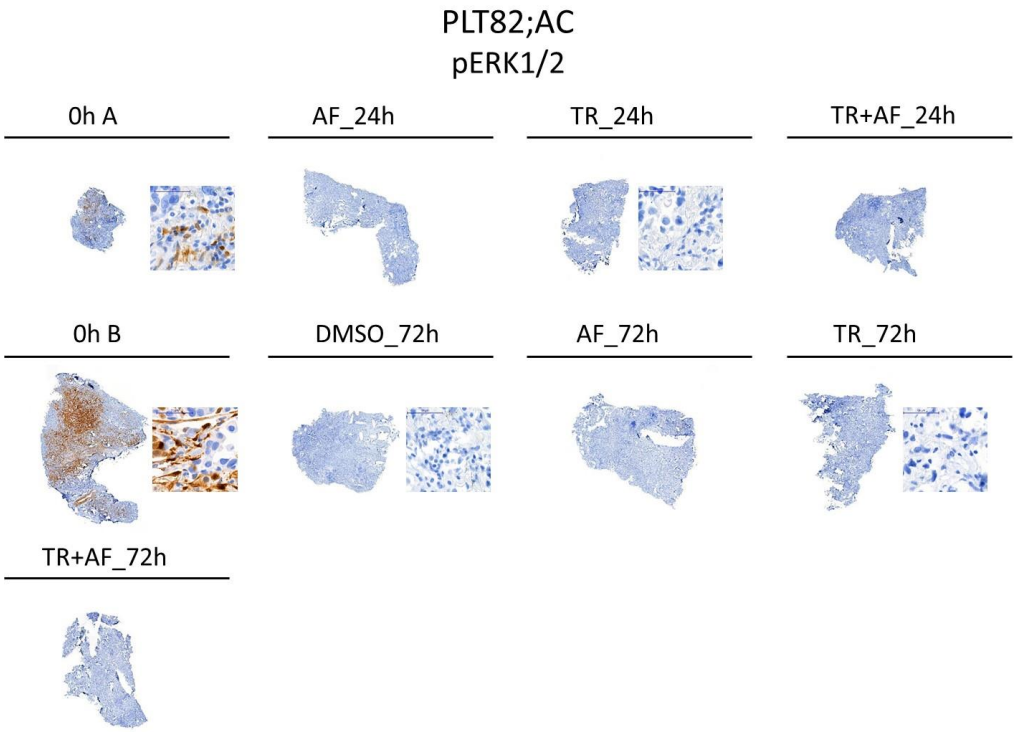

Figure 23. pERK1/2 analysis of target inactivation following TR treatment.

As a conclusion, patient-derived SCC (n=1), and AC (n=2) tissue slices were treated with TR, AF or TR+AF for 24 h or 72 h and then analyzed for cytostatic (Ki-67 positivity) and cytotoxic (CC3 positivity) response. Quantification of the viable cells is challenging due to a lot of stroma and matrix component. No significant cytotoxic or cytostatic responses were visible in the drug treated samples when compared to DMSO-treated. There was altered EGFR and ERBB2 activation in the DMSO-treated samples compared to 0 h.

9 Discussion

We only got three patient sample during our practical training, and unfortunately two of those were too soft to be sliced with Leica VT 1200S. If the tissue is too soft it escapes from the blade and does not get sliced with this technique. There can be many reasons why the tissue may be too soft for slicing, for example depending on the tumor type and tissue structure. Therefore, we did the drug treatment and culturing only for one patient sample. The Verschuren group had previously done the culturing and drug treatment for three other patient samples and processed tissue slices to FFPE blocks. Due to the lack of patient samples we also got murine tissue samples, which the Verschuren group had treated with targeted drugs and processed following the same protocol as patient samples. We sectioned and stained these samples and analyzed the results with different software, we used for example CL2M software to machine learning. One of the previously processed patient samples was so necrotic that we did not included it in our thesis.

9.1 Conclusions and development ideas

Statistical analyses were not easy to perform as we did not have a lot of samples and the results were not very consistent with each other. It was quite difficult to compare the results to each other as murine and human samples showed partly different drug responses and some of the samples were treated with different AF drug concentrations and some had different treatment times.

We did not include pAKT stained tissues in this study because all the stains were negative. We only used negative control slide for the staining, therefore we cannot be completely certain if the antibody has worked accordingly and all the pAKT samples were

actually negative. However, for other stains we also used only negative controls, in the same way as the Verschuren group usually does. With other stains, every time some of the samples were positive, hence we can assume that other antibodies have worked as they should.

For the future we think that the research should be continued with human samples as the drug responses appeared to differ between human and murine lung cancer tissue slices. Of course, the number of samples tested here was low thus no further conclusions can be drawn from this thesis alone. Murine and human lung cancer samples do correlate with each other, but not in all aspects and the results differ quite much.

9.2 Reliability and research ethics

There is plenty of previous studies about the effects of certain drugs on cancer tissue. Some of the studies that we have found have been carried out by reporting the effects of targeted drug treatments after patients have been treated (Kris et al. 2014) and some studies have used mice (Närhi et al. 2018) and cell cultures (Ekert et al. 2014) to find out the effects of the drugs. Cell cultures are cellular models that are mimicking physiologic of the tissues (Ekert et al. 2014). However, some studies that used murine tissue slices, cultured and treated *ex vivo*, have found out that tissue slices ability to mimic the *in situ* spatial heterogeneity makes them a useful complement to cell lines, which are more stable but on the other hand so uniform (Närhi et al. 2018). Therefore, it was relevant to study more about the effects of driver gene targeted drugs on surgically resected human lung cancer tissue slices and murine lung cancer tissue slices.

However, some other studies have found out that patients treated with targeted therapies have showed good response at first but later ended up with disease progression, when treated with single-agent therapy (Daga et al. 2015). Inhibiting one pathway may cause activation of other pathway, which can cause decrease of effectiveness of single-agent therapies (Hiroki et al. 2018). Therefore, development of better therapeutic strategies for lung cancer is needed, and different combinatorial treatments is required to be studied.

The murine results of this thesis were quite consistent with the Verschuren group study, which was conducted *in vivo* and *in vitro* (Talwelkar et al. 2019). For example, both our *ex vivo* and Talwelkar et al. (2019) *in vitro* results showed reduced pERK activity. Also, consistent with *in vivo* treatment results, KP;AC tissue slices showed lack of cytotoxic

response following single agent TR, AF or their combinational treatment Our human AC samples showed modest, yet not significant, increase in CC3 positivity. CC3 positivity was also increased in one of our KL;ASC samples consistent with Talwelkar et al. (2019) although our other two KL;ASC samples showed no significant increase in CC3 positivity.

With this thesis, good scientific practice was followed. We did not need our own research license. In the Verschuren group, the patient sample ethical permit work is assigned to the lab and at the lab we worked under the supervision of people who were approved for animal work. They have obtained ethical permit approval from the Coordinating Ethics Committee. We worked by following these ethical guidelines, for example patient samples were labeled with running numbers. The Verschuren group also have licensed approval to biobank patient samples in the Academic Medical Center Helsinki Biobank. All the study-enrolled patients sign an informed consent form which includes participants' rights to get study insights or cancel their study participation. Therefore, the human dignity and self-determination was preserved. Results from the project will be discussed and communicated with a team of clinical collaborators.

Mice were kept at the animal shelter, where animal attendant took care of their feeding, cleaning the cage etc. In Finland animal testing is strictly supervised. The law about animal testing 62/2006 defines who can carry out animal testing and under what kind of conditions (Laki koe-eläintoiminnasta 26/2006 § 5 & § 6). The Verschuren group have permit for animal experiments from the Finnish National Board of Animal Experimentation (Talwelkar et al 2019). In this study all the samples were treated with respect.

Participation in the workshops increased the ability to critically search the background material for this thesis. It helped us to find information more related to our thesis subject and have learned to find more good quality sources. As a database, we mainly used PubMed for information retrieval, where we found scientific articles that supported the material searching for the thesis. We received a lot of information from the research group and read their previous studies related to our thesis subject. Turnitin was used to assess and avoid plagiarism. We used source references to show where the information we used is from.

9.3 Professional growth

We started our bachelor thesis process at the beginning of January 2019. The whole process started with planning of the thesis work which was done in early spring. Making a thorough thesis plan helped us to understand the subject and made it easier to get an overall picture of this field. As the project went forward it was easier to understand detailed information when the groundwork was done properly.

The laboratory work itself was carried out during our practical training from March to June 2019 with the Verschuren group. We learned the sample workflow and carried out the slicing protocol, processing, embedding, sectioning, staining (H&E and IHC), and analysing the results, with the support and guidance from the research group members. Due to the lack of samples coming to the laboratory, we also included murine samples in this thesis project, as we mostly worked with them. We learned to do the image analysis including the machine learning and quantification of viable and dead cells. We followed the given instructions and learned to do a lot of different laboratory work and improved our technical skills.

This thesis project and working environment in our practical training have provided us a versatile perspective on lung cancer research. Working on this thesis has been incredibly interesting and we were fascinated to get to know the theory behind it in a deeper level. This experience has got us interested on working in a research laboratory. The whole process has expanded our professional abilities and we have learned many different things. We gained further knowledge of histological laboratory practises and technologies which will be useful in the future.

10 Acknowledgements

We liked to express our deepest gratitude to everyone who have helped us to complete this thesis. We are so grateful that we had an opportunity to work as a part of the Verschuren group and to do our thesis for so interesting and important topic. We give our thanks to the whole Verschuren group; to Emmy Verschuren who gave us this subject, to Ashwini Nagaraj who helped us through the whole process and to make final conclusions, to Jie Bao who helped us with picture processing and machine learning, to

Nora Linnavirta and Annabrita Schoonenberg who have teached us how to process the tissues and to do staining protocols, and to Sarang Talwelkar who helped us to understand better the cellular signaling pathways and how different drugs effect on those. We are also thankful for all the guidance we have got from our thesis supervising senior lecturer Elina Hotanen from Metropolia University of Applied Sciences.

References

Arteaga, C.and Engelmann, J. (2014). ERBB Receptors: From Oncogene Discovery to Basic Science to Mechanism-Based Cancer Therapeutics. *Cancer Cell*, 25(3), 282-303.

Asati, V., Mahapatra, D. and Bharti, S. (2016). PI3K/Akt/mTOR and Ras/Raf/MEK/ERK signalling pathways inhibitors as anticancer agents: Structural and pharmacological perspective. *European Journal of Medicinal Chemistry*, 109 (2016). 314-341.

Baik, C., Myall, N. and Wakelee, H. (2017). Targeting BRAF-Mutant Non-Small Cell Lung Cancer: From Molecular Profiling to Rationally Designed Therapy. *The Oncologist,* 22 (7). 786–796.

Bancroft, J. and Layton, C. (2013) Commitment. In S. K. Suvarna, C. Layton, J. D. Bancroft. *Bancroft's Theory and Practice of Histological Techniques.* Churchill Livingstone: Elsevier Limited.

Bao, Jie (2019). Labmeeting 140619. Figure 9. **PowerPoint presentation.** Helsinki. 14.06.

Calles, A., Sholl, L., Rodig, S., Pelton, A., Hornick, J., Butaney, M., Lydon, C., Dahlberg, S., Oxnard, G., Jackman, D. and Jänne, P. (2015). Immunohistochemical Loss of LKB1 Is a Biomarker for More Aggressive Biology in KRAS-Mutant Lung Adenocarcinoma. *Clinical Cancer Research,* 21 (12), 2851–2860.

Cancer research UK (2017). Afatinib (Giotrif). [online]. <https://www.cancerresearchuk.org/about-cancer/cancer-in-general/treatment/cancer-drugs/drugs/afatinib> Read 9.2.2019.

Cell Signaling Technology (2019a). Cleaved Caspase-3 (Asp175) (5A1E) Rabbit mAb #9664. [online] <https://www.cellsignal.com/products/primary-antibodies/cleaved-caspase-3-asp175-5a1e-rabbit-mab/9664> Read 18.8.2019.

Cell Signaling Technology (2019b). Phospho-Akt (Ser473) (193H12) Rabbit mAb #4058. [online] <https://www.cellsignal.com/products/primary-antibodies/phospho-akt-ser473-193h12-rabbit-mab/4058> Read 30.8.2019

Cell Signaling Technology (2019c). Phospho-EGF Receptor (Tyr1068) Antibody #2234. [online] <https://www.cellsignal.com/products/primary-antibodies/phospho-egf-receptor-tyr1068-antibody/2234> Read 21.8.2019

Cell Signaling Technology (2019d). Phospho-HER2/ErbB2 (Tyr1221/1222) (6B12) Rabbit mAb #2243. [online] <https://www.cellsignal.com/products/primary-antibodies/phospho-her2-erbb2-tyr1221-1222-6b12-rabbit-mab/2243> Read 27.8.2019

Cell Signaling Technology (2019e). Phospho-p44/42 MAPK (Erk1/2) (Thr202/Tyr204) (D13.14.4E) XP® Rabbit mAb #4370. [online]

<https://www.cellsignal.com/products/primary-antibodies/phospho-p44-42-mapk-erk1-2-thr202-tyr204-d13-14-4e-xp-rabbit-mab/4370> Read 21.8.2019

CKB CORE (2018). Gene Variant Detail. The Clinical Knowledgebase. [online]. <https://ckb.jax.org/geneVariant/show?geneVariantId=26327> Read 17.9.2019

Daga A., Ansari A., Patel S., Mirza S., Rawal R. and Umrania V. (2015). Current Drugs and Drug Targets in Non-Small Cell Lung Cancer: Limitations and Opportunities. *Asian Pacific Journal of Cancer Prevention*, 16 (10), 4147-4156.

Ekert, J., Johnson, K., Strake, B., Pardinas, J., Jarantow, S., Perkison, R. and Colter, D. (2014). Three-Dimensional Lung Tumor Microenvironment Modulates Therapeutic Compound Responsiveness In Vitro – Implication for Drug Development. *PLOS One,* 9 (3).

Fan, Y. and Bergmann, A. (2010). The cleaved-Caspase-3 antibody is a marker of Caspase-9-like DRONC activity in Drosophila. *Cell Death and Differentiation*, 17(3), 534-539.

Fang, W., Huang, Y., Hong, S., Zhang, Z., Wang, M., Gan, J., Wang, W., Guo, H., Wang, K. and Zhang L. (2019). EGFR exon 20 insertion mutations and response to osimertinib in non-small-cell lung cancer. *BMC Cancer*, 19, 595.

FIMM. (2019). Verschuren Lung Cancer Model Systems. [online]. <https://www.fimm.fi/en/research/groups/verschuren> Read 1.2.2018

Hers, I., Vincent, E. and Tavaré, J. (2011). Akt signalling in health and disease. *Cell Signal,* 23(10), 1515-27.

Hiroki, S., Hiromasa, Y., Masakiyo, S., Kazuhiko, S., Shuta, T., Tadahiko, S., Hirokuni, I., Minami, H., Hidejiro, T., Kei, N., Takahiro, Y., Eisuke, K., Yusuke, O., Yuta, T., Junichi, S. and Shinichi, T. (2018). Combined inhibition of MEK and PI3K pathways overcomes acquired resistance to EGFR-TKIs in non-small cell lung cancer. *Cancer Science,* 109(10), 3183-3196.

Hirsch, F., Suda, K., Wiens, J. and Bunn, P. (2016). New and emerging targeted treatments in advanced non-small-cell lung cancer. *The Lancet,* 388 (10048), 1012–1024.

Hirsch, F., Varella-Garcia, M., Bunn Jr, P., Di Maria, M., Veve, R., Bremnes, R., Barón, A., Zeng, C. and Franklin, W. (2003). Epidermal Growth Factor Receptor in Non–Small-Cell Lung Carcinomas: Correlation Between Gene Copy Number and Protein Expression and Impact on Prognosis. *Journal of Clinical Oncology*, 21, 3798-3807.

Horobin, R. (2013) Commitment. In S. K. Suvarna, C. Layton, J. D. Bancroft. *Bancroft's Theory and Practice of Histological Techniques*. Churchill Livingstone: Elsevier Limited.

Hyeong, S., Jung, H., Boram, H. and Dae, R. (2019). Correlation of Thyroid Transcription Factor-1 Expression with EGFR Mutations in Non-Small Cell Lung Cancer: A Meta-Analysis. *Medicina,* 55 (2), 41.

Jackson, P. and Blythe, D. (2013) Commitment. In S. K. Suvarna, C. Layton, J. D. Bancroft. *Bancroft's Theory and Practice of Histological Techniques: Immunohistochemical techniques*. Churchill Livingstone: Elsevier Limited.

Jiang, F and McKeegan E. M. (2015) Commitment. In S. A. Aziz and R. Mehta (eds.) *Technical Aspects of Toxicological Immunohistochemistry: Immunohistochemistry in the Study of Cancer Biomarkers for Oncology Drug Development.* New York, Springer Science + Business Media.

Kanan, Y., Matsumoto, H., Song, H., Sokolov, M., Anderson, R. and Rajala, R (2010). Serine/Threonine Kinase Akt Activation Regulates the Activity of Retinal Serine/Threonine Phosphatases, PHLPP and PHLPPL. *Journal of Neurochemistry*, 113(2), 477-488.

Knuuttila, A. (2014a) Commitment. In R. Kaarteenaho, P. Brander, M. Halme, and V. Kinnula (eds.) *Keuhkosairaudet*, Diagnostiikka. Helsinki: Kustannus Oy Duodecim.

Knuuttila, A. (2014b) Commitment. In R. Kaarteenaho, P. Brander, M. Halme, and V. Kinnula (eds.) *Keuhkosairaudet*, Hoito ja ennuste*.* Helsinki: Kustannus Oy Duodecim.

Knuuttila, A. (2014c) Commitment. In R. Kaarteenaho, P. Brander, M. Halme, and V. Kinnula (eds.) *Keuhkosairaudet,* Keuhkosyöpien etiologia. Helsinki: Kustannus Oy Duodecim.

Knuuttila, A. (2014d) Commitment. In R. Kaarteenaho, P. Brander, M. Halme, and V. Kinnula (eds.) *Keuhkosairaudet,* Keuhkosyöpien jaottelu. Helsinki: Kustannus Oy Duodecim.

Knuuttila, A. (2014e) Commitment. In R. Kaarteenaho, P. Brander, M. Halme, and V. Kinnula (eds.) *Keuhkosairaudet,* Keuhkosyövät; Johdanto. Helsinki: Kustannus Oy Duodecim.

Kris, M., Johnson, B., Berry, L., Kwiatkowski, D., Iafarate, A., Wistuba, I., Varella-Garcia, M., Franklin, W., Aronson, S., Su, P-F., Shyr, Y., Camidge, R., Sequist, L., Glisson, B., Khuri, F., Garon, E., Pao, W., Rudin, C., Schiller, J., Haura, E, Socinski, M., Shirai, K., Chen, H., Giaccone, G., Ladanyi, M., Kugler, K., Minna, J. and Bunn, P. (2014). Using Multiplexed Assays of Oncogenic Drivers in Lung Cancers to Select Targeted Drugs. *JAMA*, 311 (19), 1998–2006.

Laki koe-eläintoiminnasta 62/2006. Issued in Helsinki 20.1.2006.

Liu, P-F., Hu, Y-C., Kang, B-H., Tseng, Y-K., Wu, P-C., Liang, C-C., Hou, Y-Y., Fu, T-Y., Liou, H-H., Hsieh, I-C., Ger, L-P. and Shu, C-W. (2017). Expression levels of cleaved caspase-3 and caspase-3 in tumorigenesis and prognosis of oral tongue squamous cell carcinoma. *PLoS One*, 12(7), e0180620.

Mali, P. (2013a) Commitment. In H. Joensuu, P. J. Roberts, P-L. Kellokumpu-Lehtinen, S. Jyrkkiö, M. Kouri and L. Teppo (eds.) *Syöpätaudit,* Keuhkosyövän yleisyys. Helsinki: Kustannus Oy Duodecim.

Mali, P. (2013b) Commitment. In H. Joensuu, P. J. Roberts, P-L. Kellokumpu-Lehtinen, S. Jyrkkiö, M. Kouri and L. Teppo (eds.) *Syöpätaudit,* Keuhkosyövän patologia ja molekyylibiologia. Helsinki: Kustannus Oy Duodecim.

Mali, P. (2013c) Commitment. In H. Joensuu, P. J. Roberts, P-L. Kellokumpu-Lehtinen, S. Jyrkkiö, M. Kouri and L. Teppo (eds.) *Syöpätaudit,* Keuhkosyövän vaaratekijät. Helsinki: Kustannus Oy Duodecim.

Mebratu, Y. and Tesfaigi, Y. (2009). How ERK1/2 Activation Controls Cell Proliferation and Cell Death Is Subcellular Localization the Answer?. *Cell Cycle*, 8(8), 1168-1175.

MedlinePlus (2018). Trametinib. [online]. <https://medlineplus.gov/druginfo/meds/a613040.html> Read 9.2.2019

Moon, A (2013) Commitment. In S. K. Suvarna, C. Layton, J. D. Bancroft. Bancroft's *Theory and Practice of Histological Techniques.* Churchill Livingstone: Elsevier Limited.

Mäkinen, M. (2012) Commitment. In M. Mäkinen, O. Carpén, V-M. Kosma, V-P. Lehto, T. Paavonen, and F. Stenbäck (eds.) *Patologia*, Näytteiden käsittely laboratoriossa. Helsinki: Kustannus Oy Duodecim.

Mäkinen, M. and Stenbäck, F. (2012a) Commitment. In M. Mäkinen, O. Carpén, V-M. Kosma, V-P. Lehto, T. Paavonen, and F. Stenbäck (eds.) *Patologia,* Immunohistokemia diagnostiikan apuvälineenä*.* Helsinki: Kustannus Oy Duodecim.

Mäkinen, M. and Stenbäck, F. (2012b) Commitment. In M. Mäkinen, O. Carpén, V-M. Kosma, V-P. Lehto, T. Paavonen, and F. Stenbäck (eds.) *Patologia,* Immunohistokemialliset menetelmät. Helsinki: Kustannus Oy Duodecim.

Mäkinen, M. and Stenbäck, F. (2012c) Commitment. In M. Mäkinen, O. Carpén, V-M. Kosma, V-P. Lehto, T. Paavonen, and F. Stenbäck (eds.) *Patologia,* Vasta-aineet. Helsinki: Kustannus Oy Duodecim.

Nagaraj, A., Bao, J., Hemmes, A., Machado, M., Närhi, K. and Verschuren, E. (2018). Establishment and Analysis of Tumor Slice Explants As a Prerequisite for Diagnostic Testing. *Journal of Visualized experiments: JoVE (*141).

Nagaraj, A., Lahtela, J., Hemmes, A., Pellinen, T., Blom, S., Devlin, J., Salmenkivi, K., Kallioniemi, O., Mäyränpää, M., Närhi, K. and Verschuren, E. (2017). Cell of Origin Links Histotype Spectrum to Immune Microenvironment Diversity in Non-small-Cell Lung Cancer Driven by Mutant Kras and Loss of Lkb1. *Cell Reports* 18 (3), 673-684.

National Cancer Institute (2019a). Afatinib (Code C66940). [online]. <https://ncit.nci.nih.gov/ncitbrowser/ConceptReport.jsp?dictionary=NCI_Thesaurus&ns=NCI_Thesaurus&code=C66940> Read 9.2.2019.

National Cancer Institute (2019b) Trametinib (Code C77908). [online]. <https://ncit.nci.nih.gov/ncitbrowser/ConceptReport.jsp?dictionary=NCI_Thesaurus&ns=NCI_Thesaurus&code=C77908> Read 9.2.2019.

Network Genomic Medicine Lung Cancer (2016). *Driver mutations in lung cancer* [online]. <https://ngm-cancer.com/en/driver-mutations/> Read 9.2.2019

Närhi, K., Nagaraj, A., Parri, E., Turkki, R., W van Dujin, P., Hemmes, A., Lahtela, J., Uotinen, V., Mäyränpää, M., Salmenkivi, K., Räsänen, J., Linder, N., Tarpman, J., Rannikko, A., Kallioniemi, O., Hällström, T., Lundin, J., Sommergruber, W., Anders, S. and Verschuren, E. (2018). Spatial aspects of oncogenic signalling determine the response to combination therapy in slice explants from Kras-driven lung tumours. *The Journal of Pathology*, 245 (1), 101-113.

O'Hagan, R. and Heyer, J. (2011). KRAS Mouse Models. *Genes & Cancer,* 2 (3), 335–343.

Pillai, R., Behera, M., Berry, L., Rossi, M., Kris, M., Johnson, B., Bunn, P., Ramalingam, S.and Khuri, F. (2017). HER2 Mutations in Lung Adenocarcinoma: A Report from the Lung Cancer Mutation Consortium. *Cancer,* 123 (21), 4099-4105.

Ren, X. and Malik, J. (2003). Learning a classification model for segmentation. Institute of Electrical and Electronics Engineers. [online] <https://ieeexplore.ieee.org/abstract/document/1238308> Read 8.11.2019

Rhodes, A (2013) Commitment. In S. K. Suvarna, C. Layton, J. D. Bancroft. *Bancroft's Theory and Practice of Histological Techniques.* Churchill Livingstone: Elsevier Limited.

Sanderson, T. and Zardin, G. (2013) Commitment. In S. K. Suvarna, C. Layton, J. D. Bancroft. *Bancroft's Theory and Practice of Histological Techniques.* Churchill Livingstone: Elsevier Limited.

Spencer, L. and Bancroft, J. (2013) Commitment. In S. K. Suvarna, C. Layton, J. D. Bancroft. *Bancroft's Theory and Practice of Histological Techniques.* Churchill Livingstone: Elsevier Limited.

Suvarna, S. and Layton, C. (2013) Commitment. In S. K. Suvarna, C. Layton, J. D. Bancroft (eds.) *Bancroft's Theory and Practice of Histological Techniques.* Churchill Livingstone: Elsevier Limited.

Talwelkar, S., Nagaraj, A., Devlin, J., Hemmes, A., Potdar, S., Kiss, E., Saharinen, P., Salmenkivi, K., Mäyränpää, N., Wennerberg, K. and Verschuren, E. (2019). Reseptor Tyrosine Kinase Signaling Networks Define Sensitivity to ERBB Inhibition and Stratify Kras-Mutant Lung Cancers. *Molecular Cancer Therapeutics,* 18 (10), 1863-1874.

Talwelkar, Sarang (2019): *Patient sample collection and ethical approval*. Private email message 22.2.2019. Research group's own material.

Thermo Fischer Scientific a. Lab Vision™ Ki-67, Rabbit Monoclonal Antibody. [online] <https://www.thermofisher.com/order/catalog/product/RM-9106-R7> Read 27.8.2019

Thermo Fisher Scientific b. Antigen or Epitope Retrieval Methods for IHC. [online]. <https://www.thermofisher.com/fi/en/home/life-science/protein-biology/protein-biology-learning-center/protein-biology-resource-library/pierce-protein-methods/paraffin-removal-antigen-retrieval.html#1> Read 7.9.2019.

Verheijen, M., Lienhard, M., Schrooders, Y., Clayton, O., Nudischer, R., Boerno, S., Timmermann, B., Selevsek, N., Schlapbach, R., Gmuender, H., Gotta, S., Geraedts, J., Herwig, R., Kleinjans, J. and Caiment, F. (2019). DMSO induces drastic changes in human cellular processes and epigenetic landscape in vitro. *Scientific Reports*, 9 (1), 4641.

Vijayalakshmi, R. and Krishnamurthy, A. (2011). Targetable “Driver” Mutations in Non Small Cell Lung Cancer. *Indian Journal of Surgical Oncology,* 2(3), 178-188.

Young, B., Stewart, W. and O’Down, G. (2011). *Wheater’s Basic Pathology A Text, Atlas and Review of Histopathology.* Churchill Livingstone: Elsevier Limited.

Murine sample KL;ASC T1 050618 results

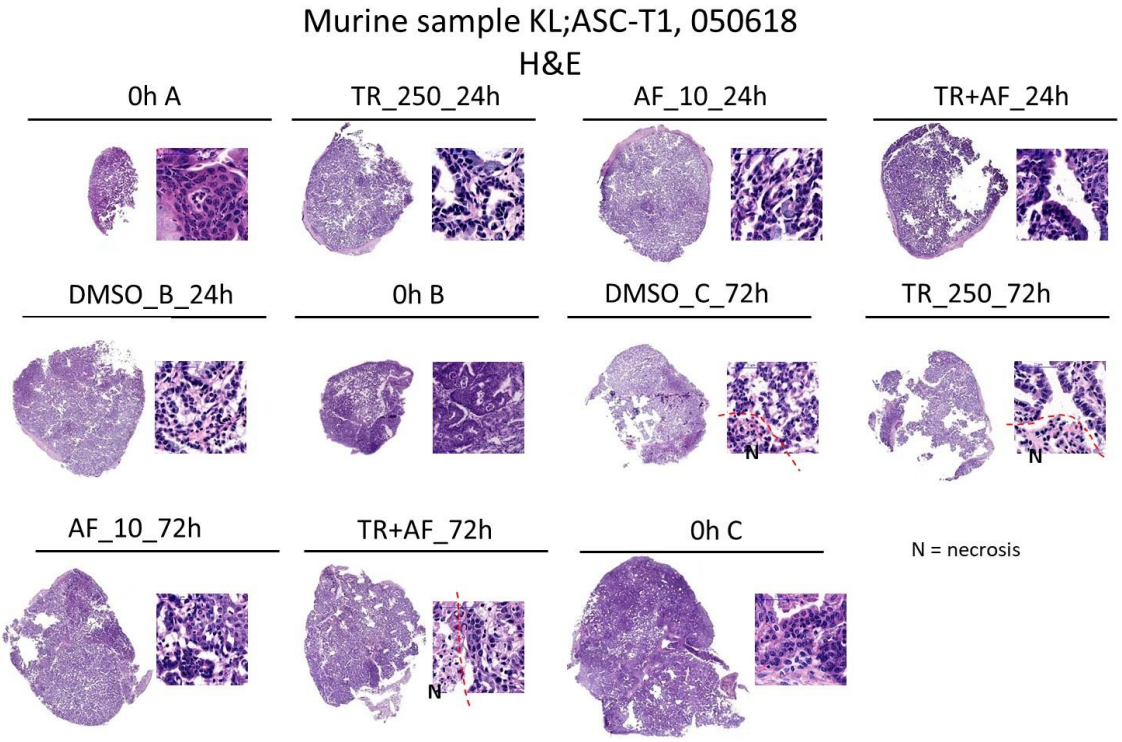

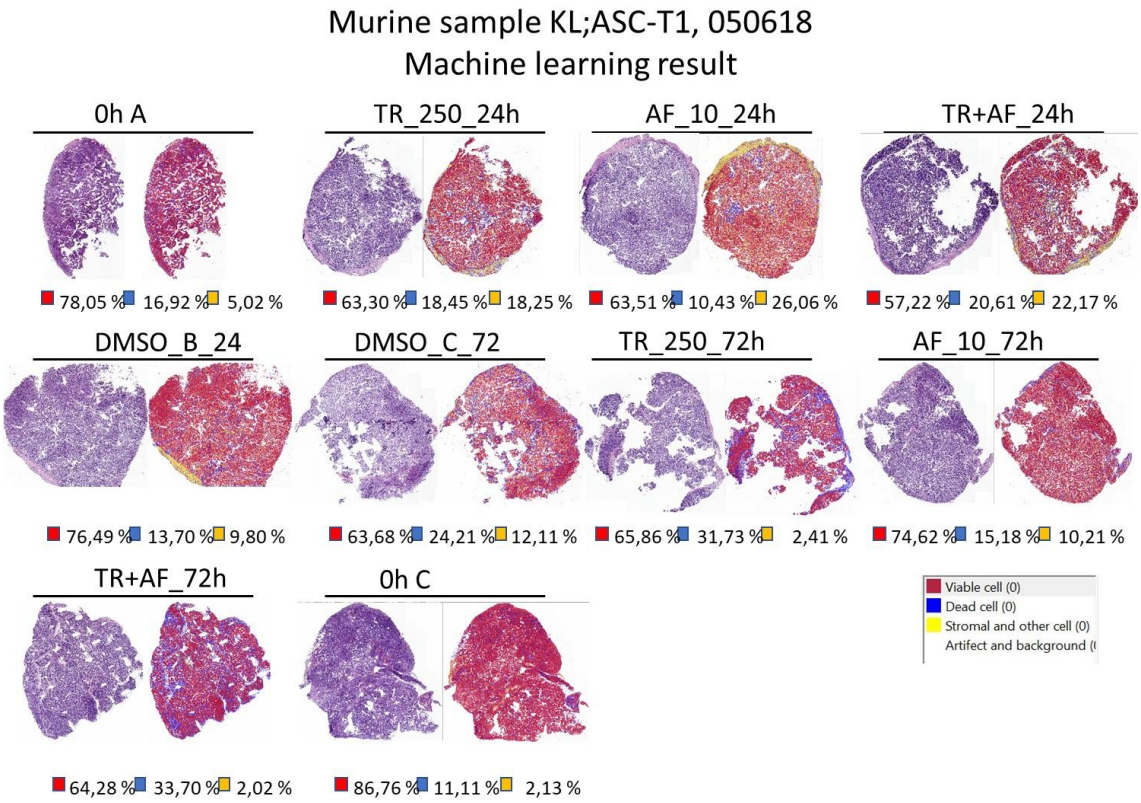

Murine sample KL;ASC-T1, 050618
CC3

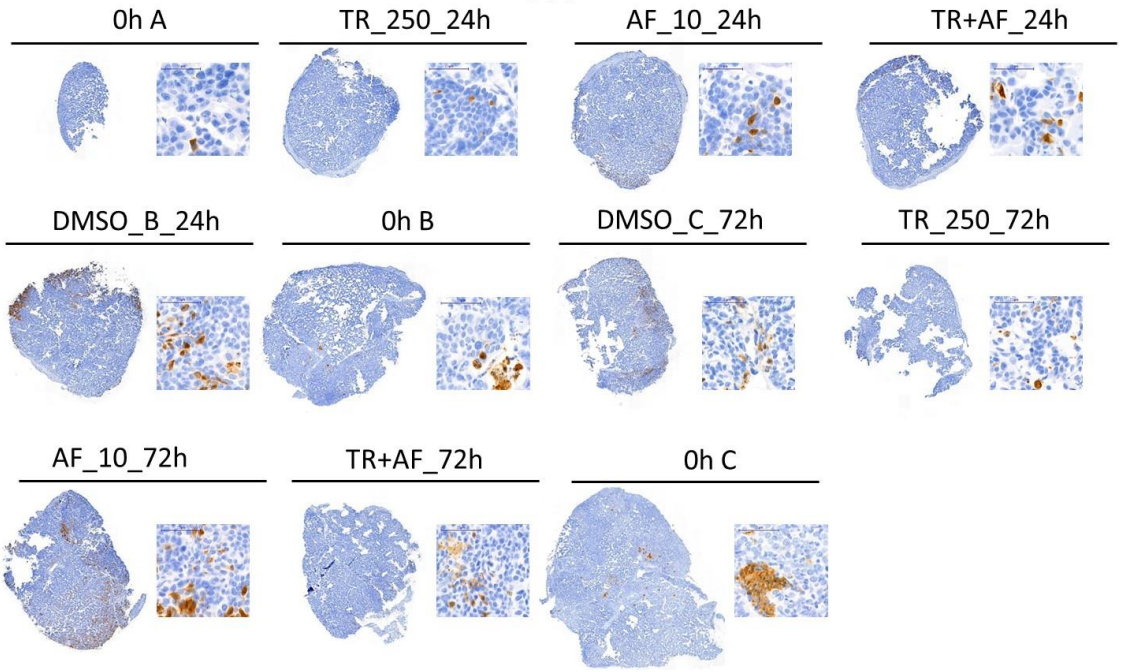

Murine sample KL;ASC-T1, 050618
Ki-67

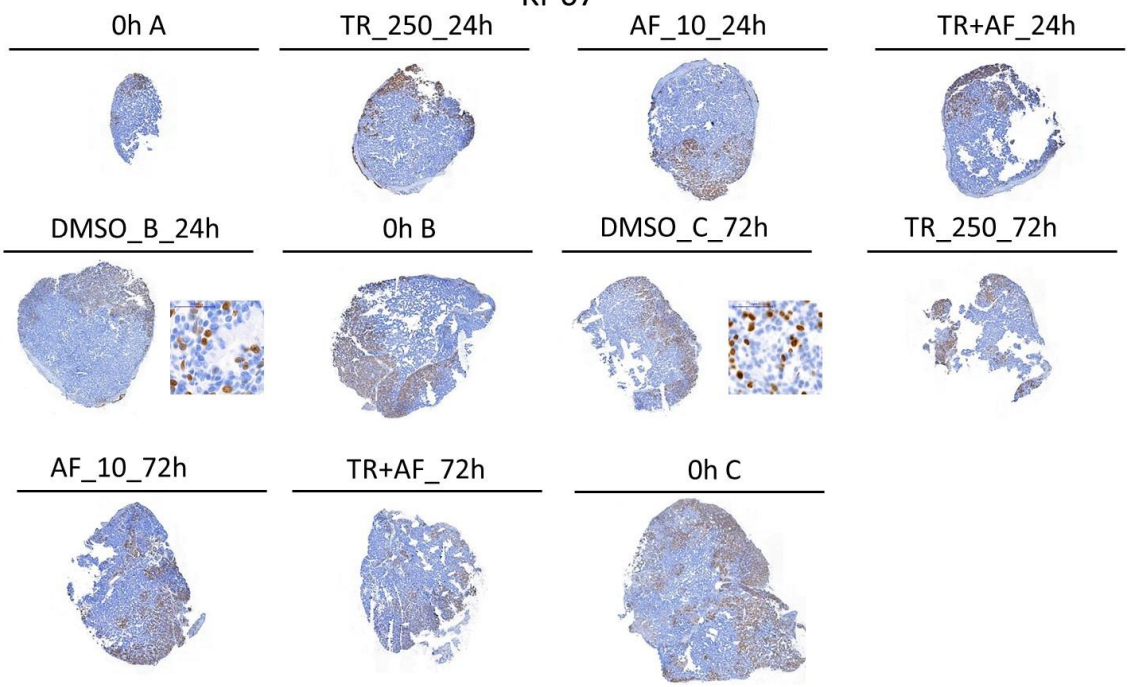

Murine sample KL;ASC-T1, 050618
pERBB2

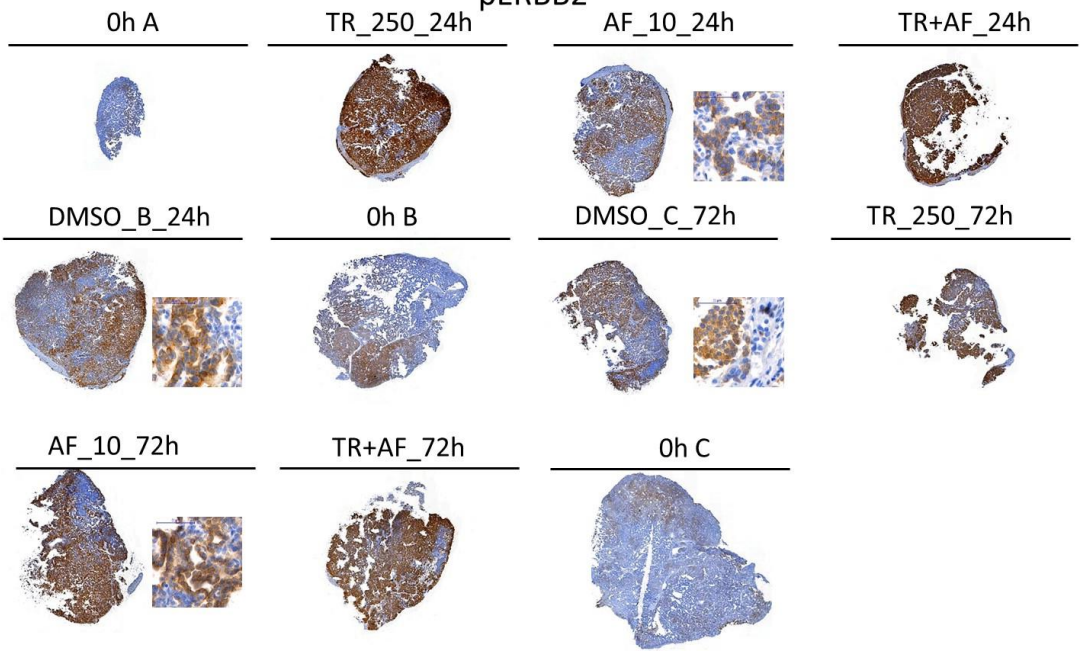

Murine sample KL;ASC-T1, 050618
pERK1/2

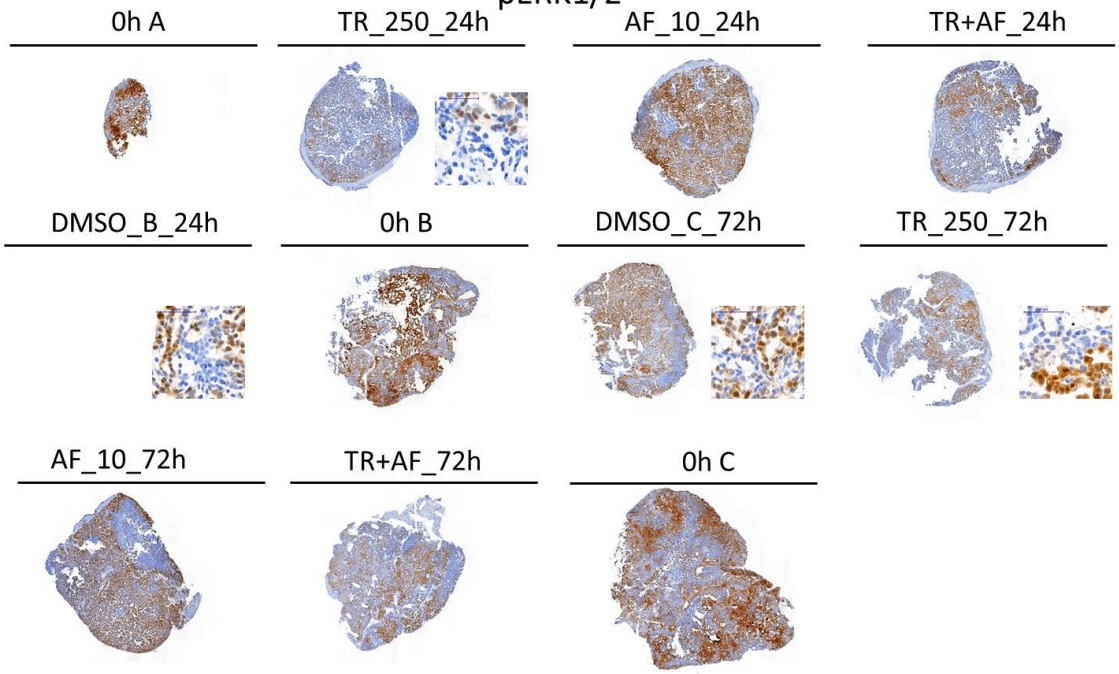

Murine sample KL;ASC T2 050618 results

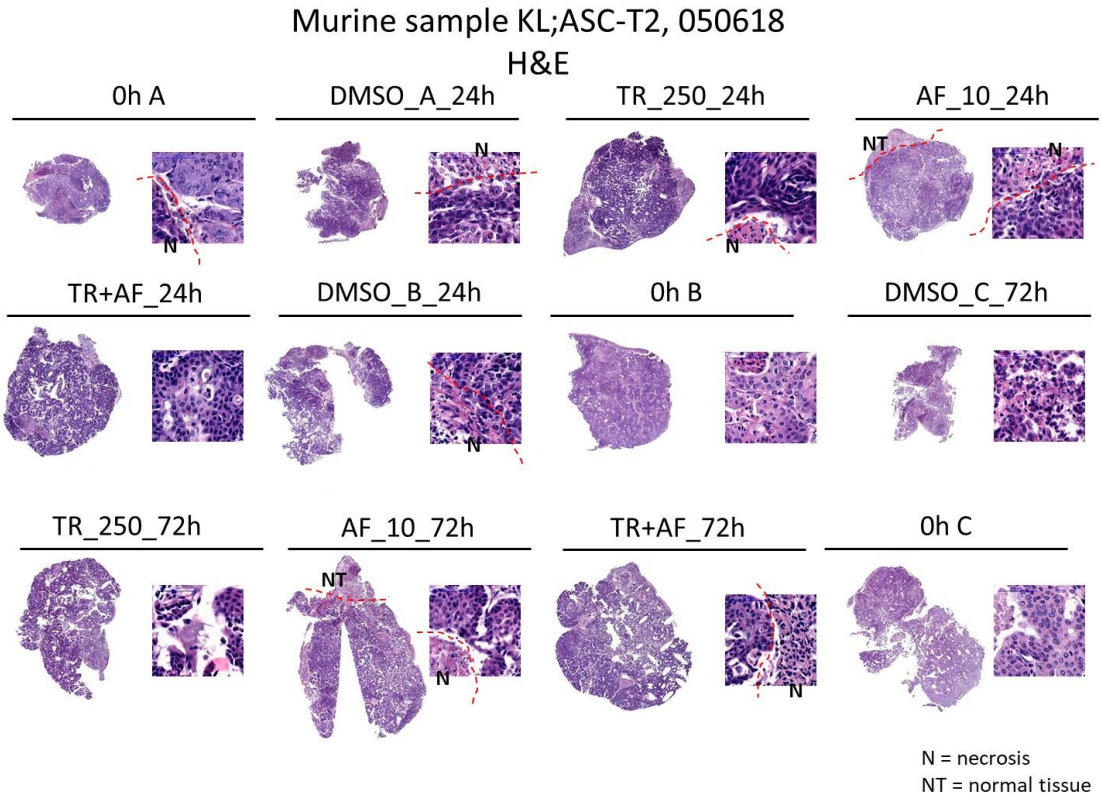

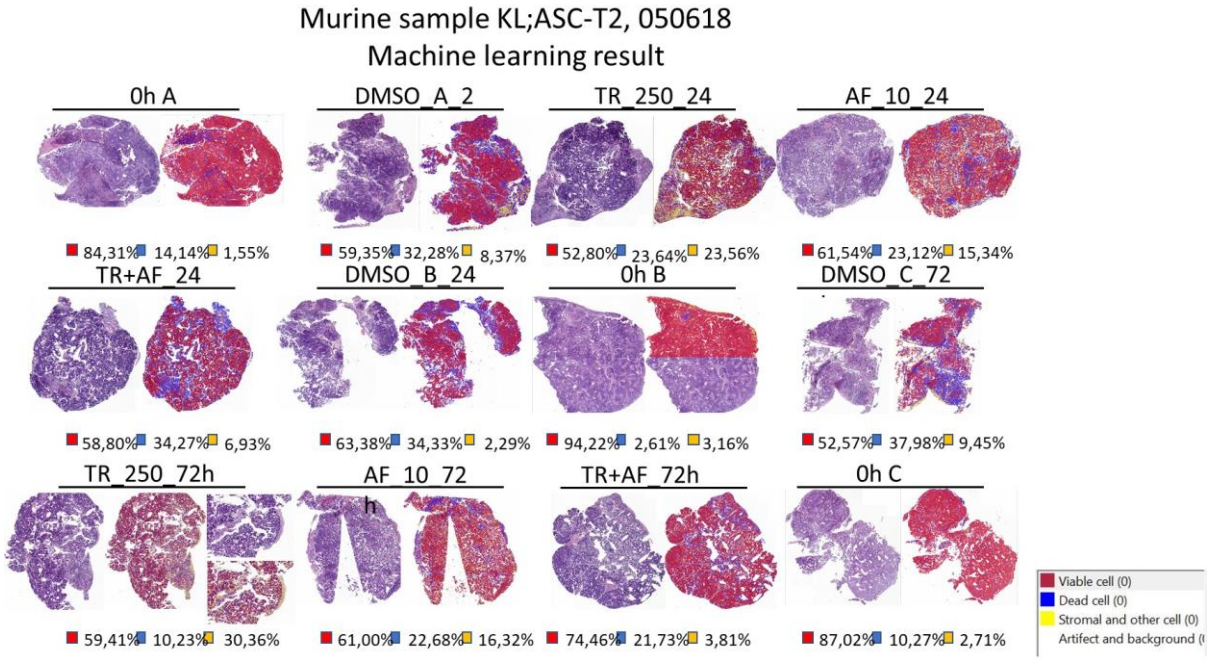

Murine sample KL;ASC-T2, 050618
CC3

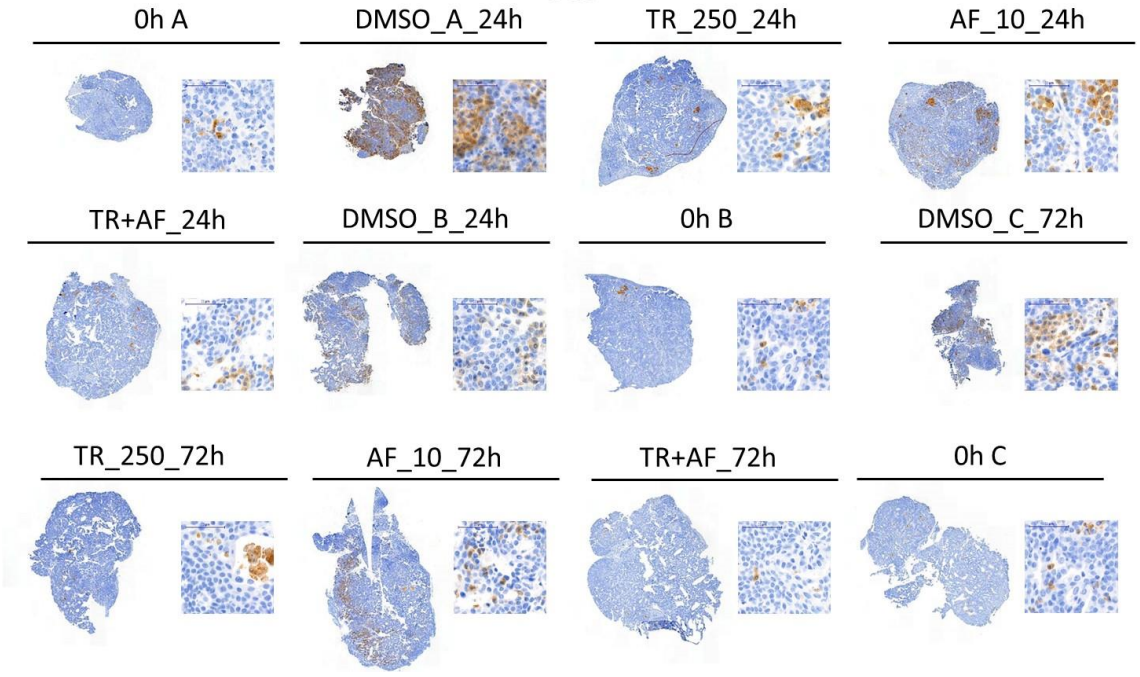

Murine sample KL;ASC-T2, 050618
Ki-67

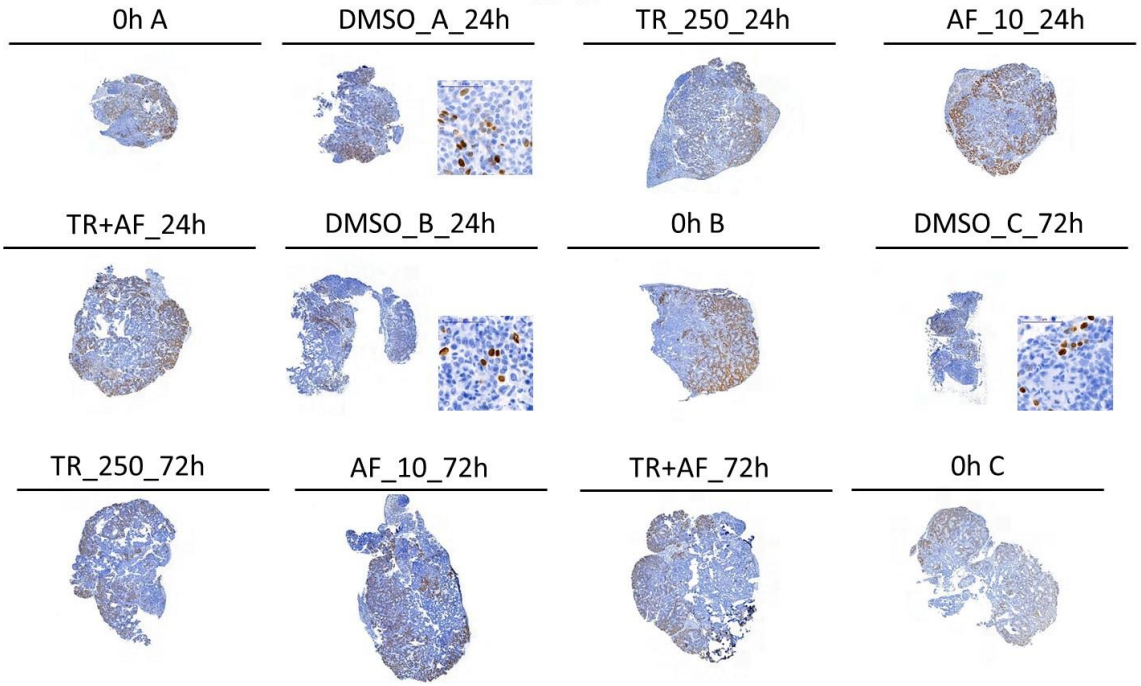

Murine sample KL;ASC-T2, 050618
pERBB2

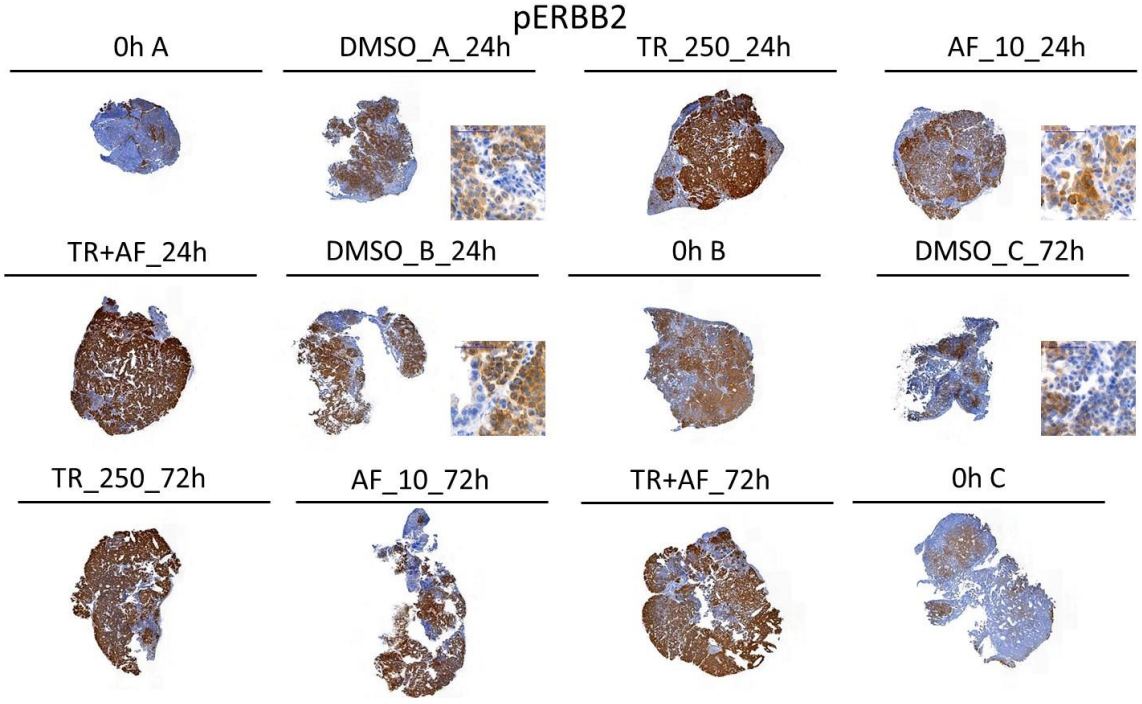

Murine sample KL;ASC-T2, 050618
pERK1/2

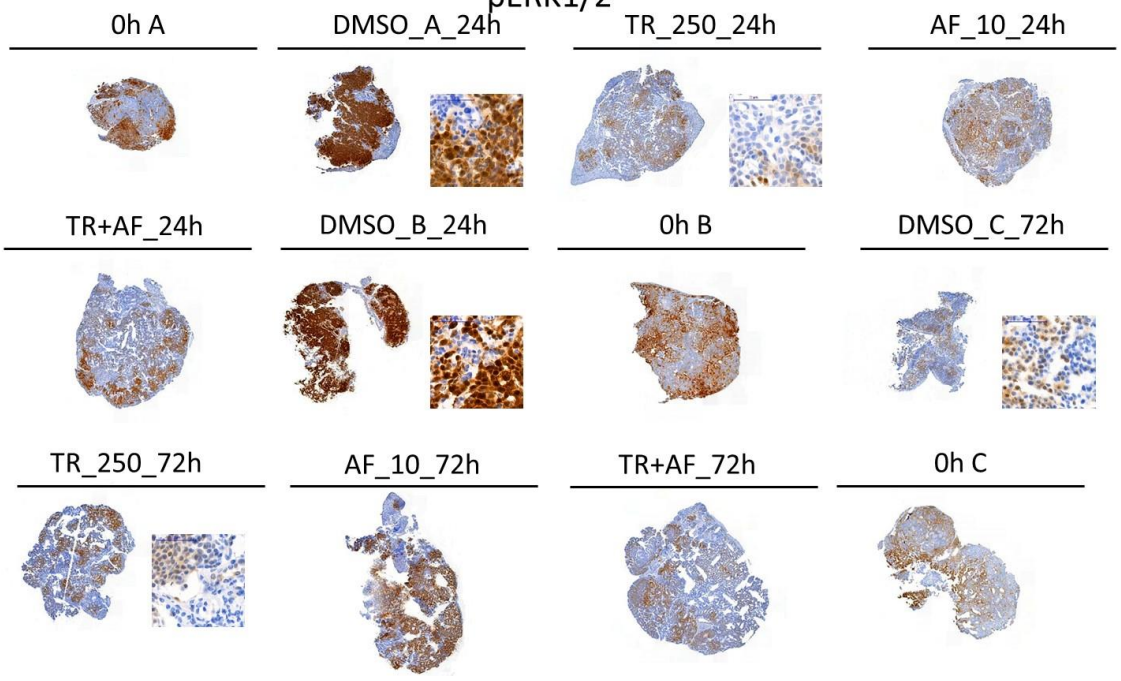

Murine sample KP;AC 311017 results

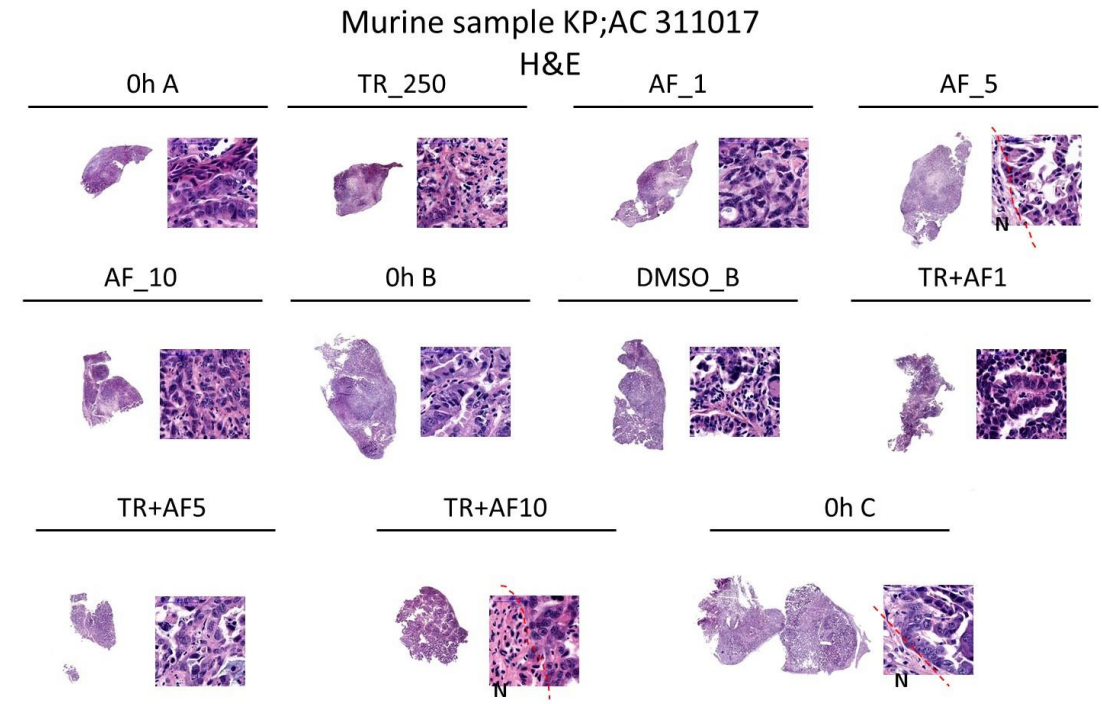

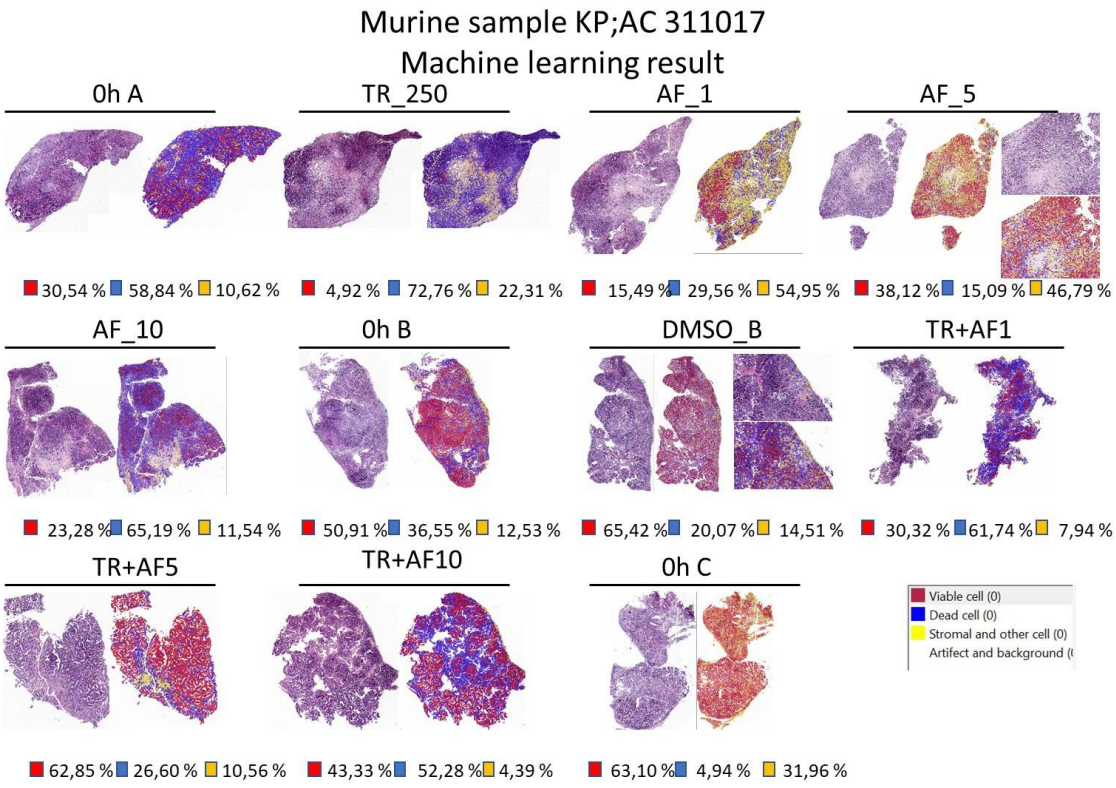

Murine sample KP;AC 311017
CC3

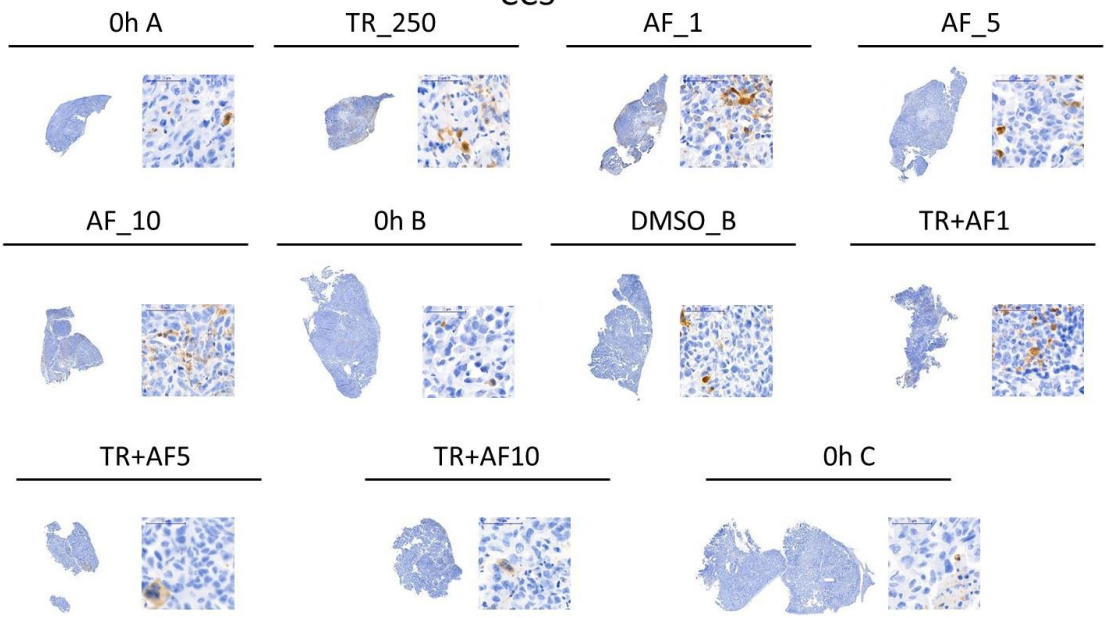

Murine sample KP;AC 311017
Ki-67

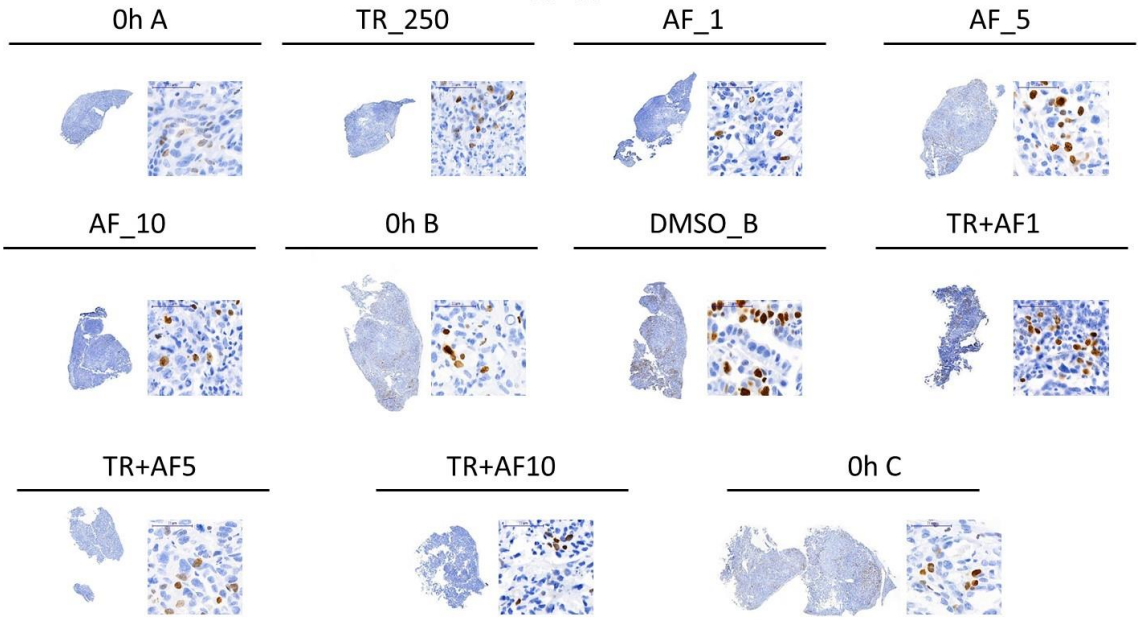

Murine sample KP;AC 311017
pERBB2

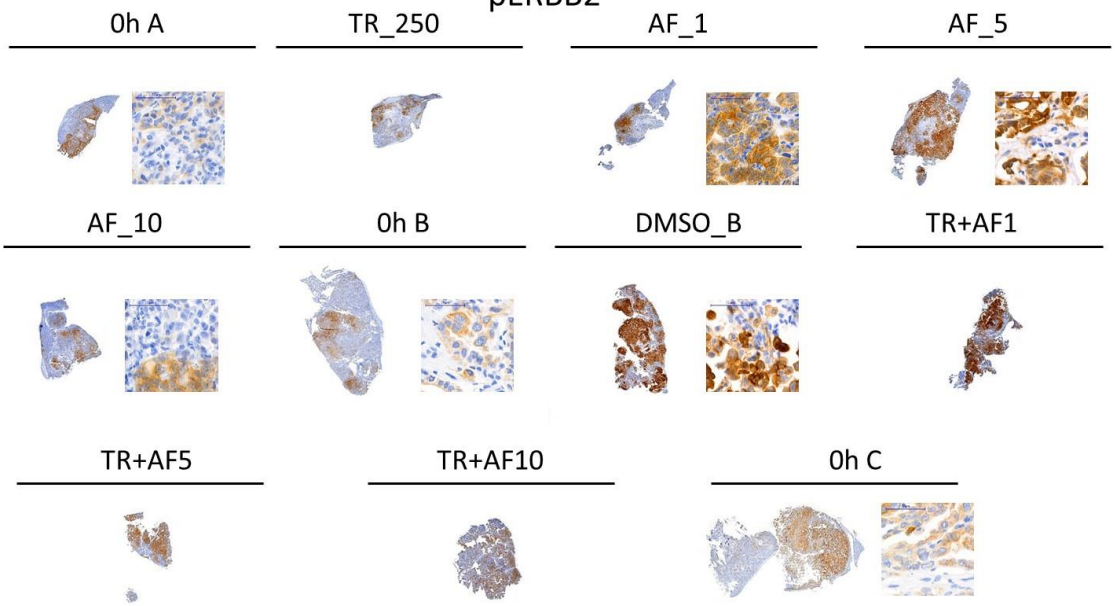

Murine sample KP;AC 311017
pERK1/2

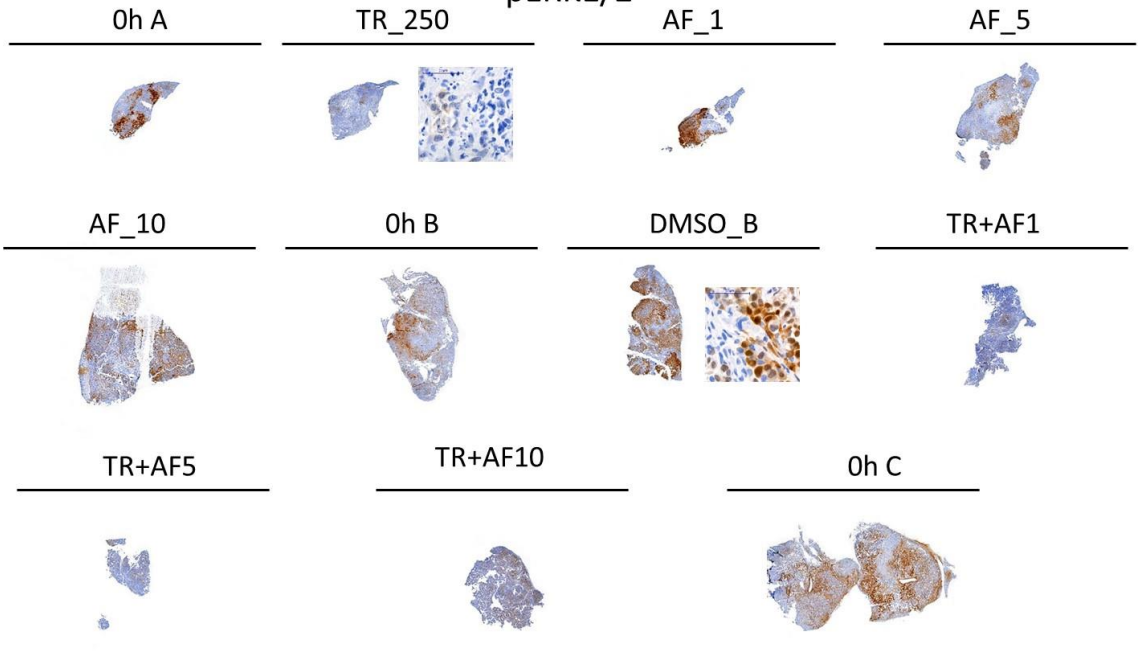

Human sample PLT76;SCC results

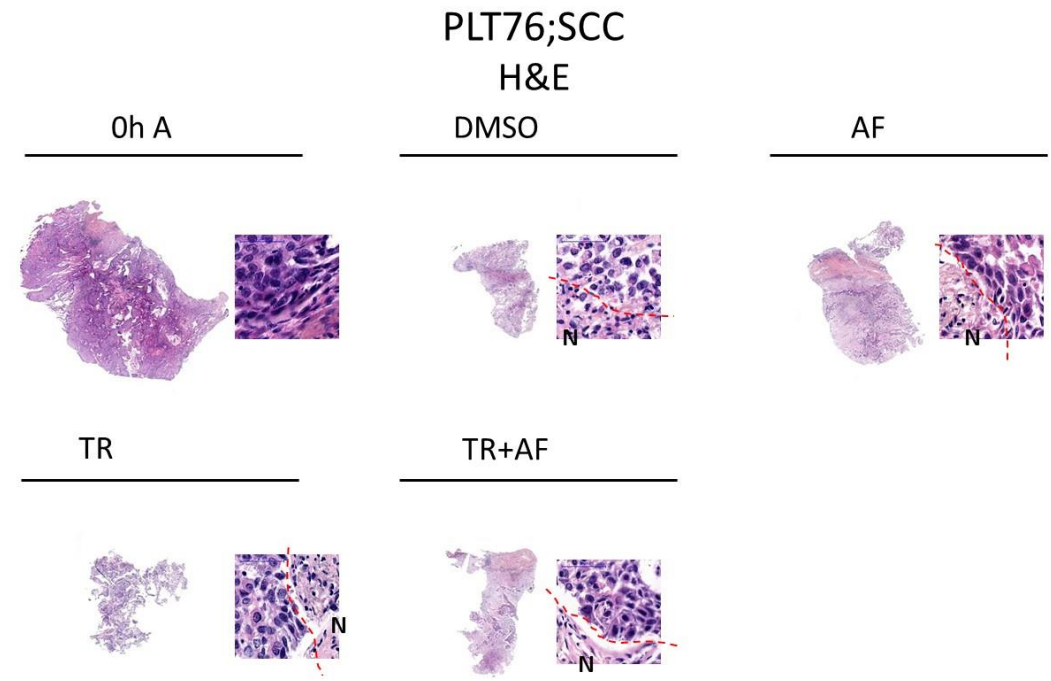

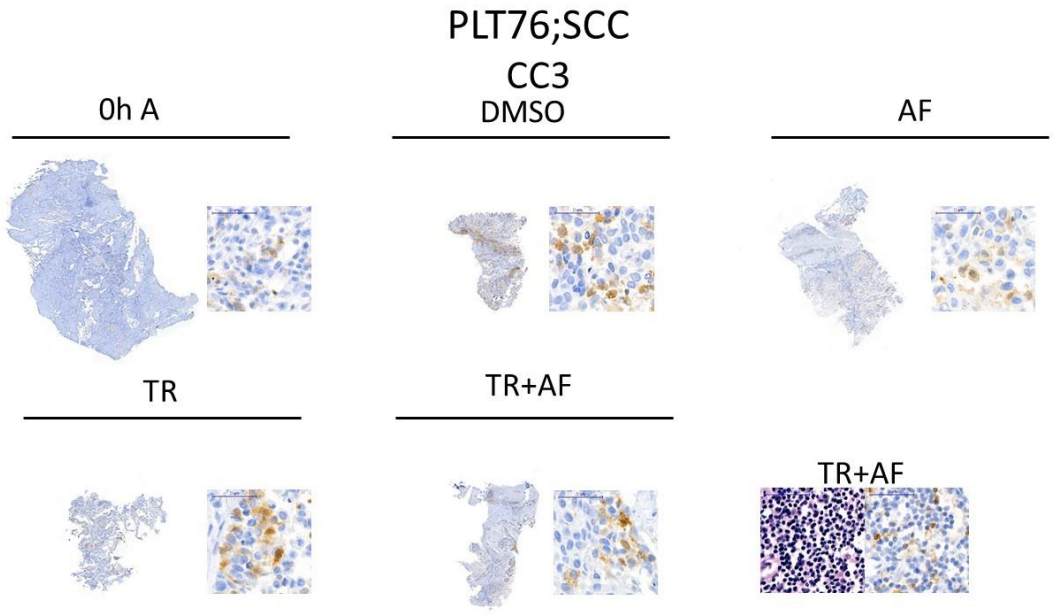

PLT76;SCC
Ki-67

0h A

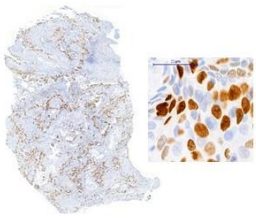

DMSO

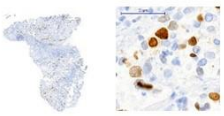

AF

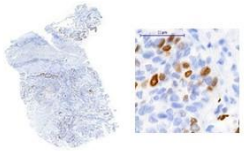

TR

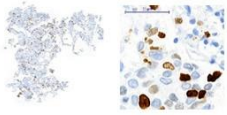

TR+AF

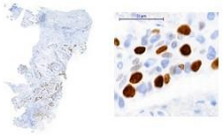

PLT76;SCC
pEGFR

0h A

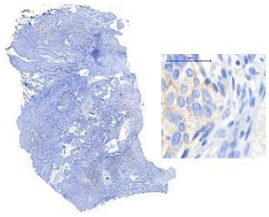

DMSO

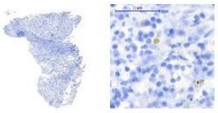

AF

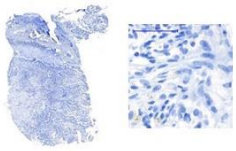

TR

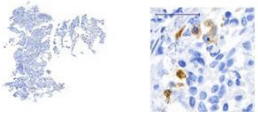

TR+AF

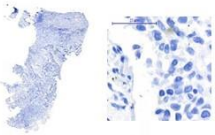

PLT76;SCC
pERBB2

0h A

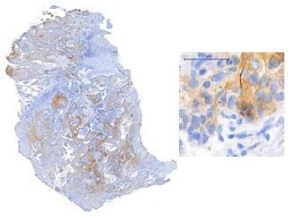

DMSO

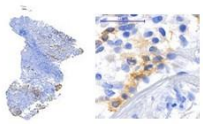

AF

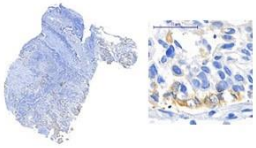

TR

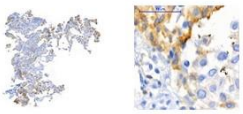

TR+AF

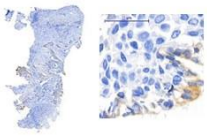

PLT76;SCC
pERK1/2

0h A

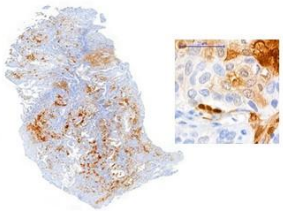

DMSO

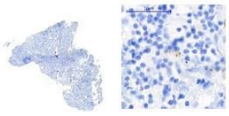

AF

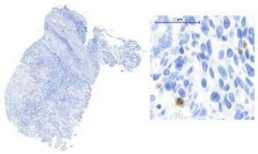

TR

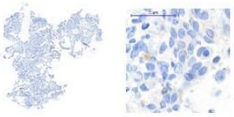

TR+AF

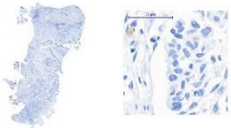

Human sample PLT73;AC results

PLT73;AC
H&E

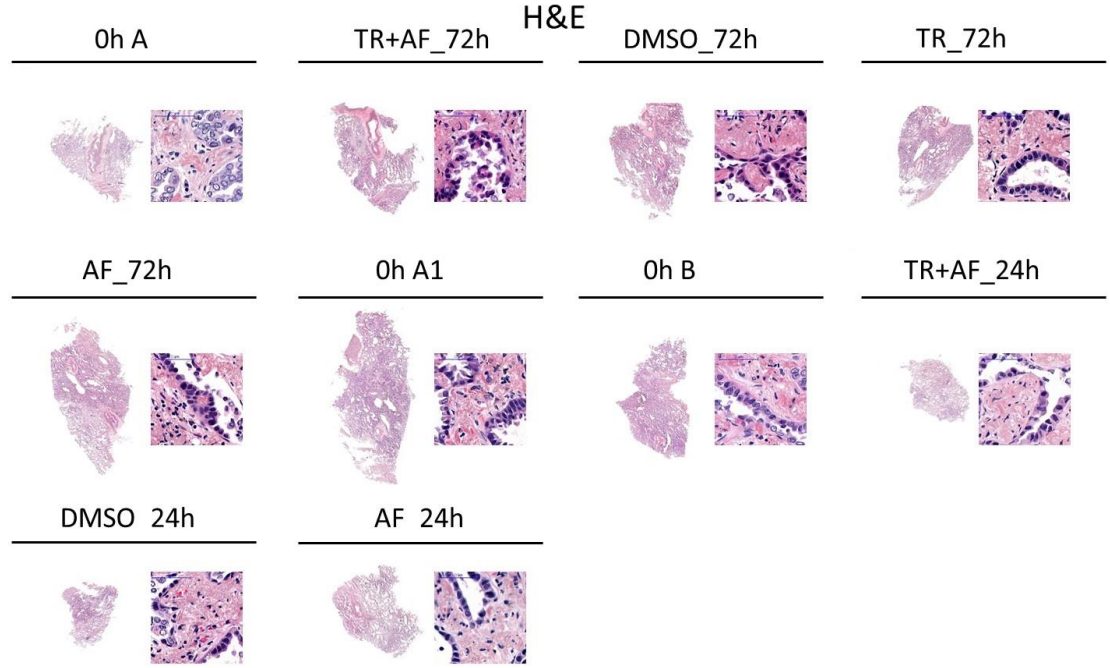

PLT73;AC
CC3

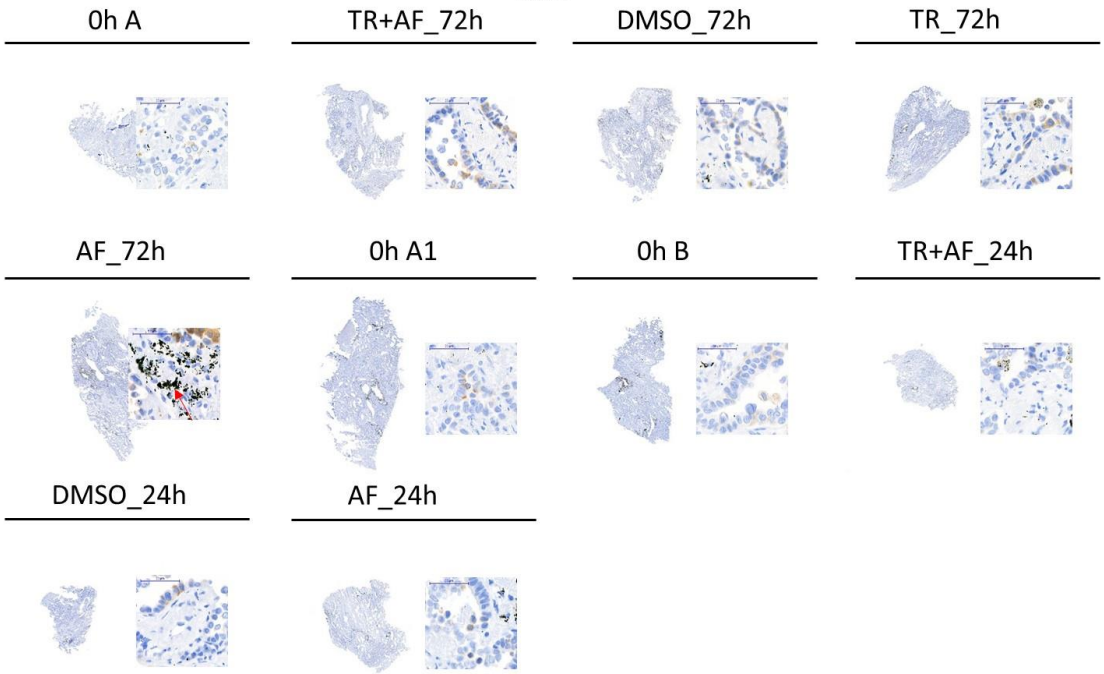

PLT73;AC
Ki-67

0h A

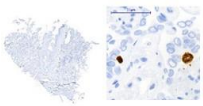

TR+AF_72h

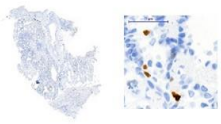

DMSO_72h

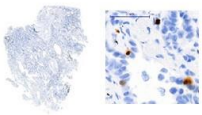

TR_72h

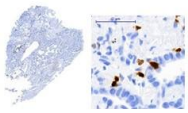

AF_72h

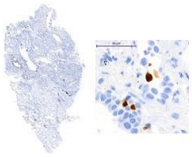

0h A1

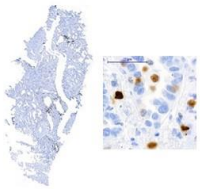

0h B

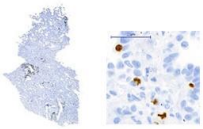

TR+AF_24h

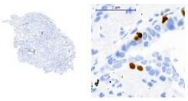

DMSO_24h

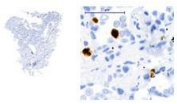

AF_24h

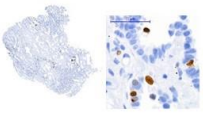

PLT73;AC
pEGFR

0h A

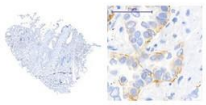

TR+AF_72h

DMSO_72h

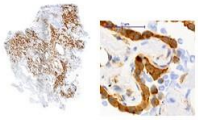

TR_72h

AF_72h

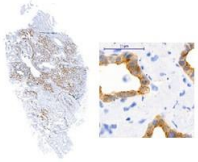

0h A1

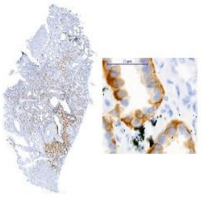

0h B

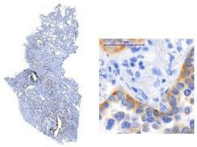

TR+AF_24h

DMSO_24h

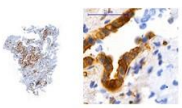

AF_24h

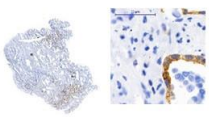

PLT73;AC
pERBB2

0h A

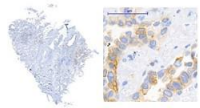

TR+AF_72h

DMSO_72h

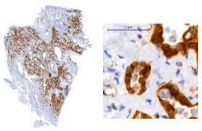

TR_72h

AF_72h

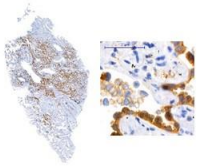

0h A1

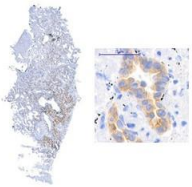

0h B

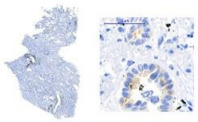

TR+AF_24h

DMSO_24h

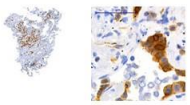

AF_24h

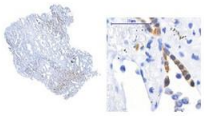

PLT73;AC
pERK1/2

0h A

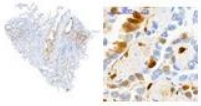

TR+AF_72h

DMSO_72h

TR_72h

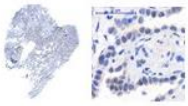

AF_72h

0h A1

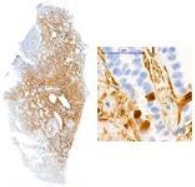

0h B

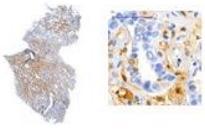

TR+AF_24h

DMSO_24h

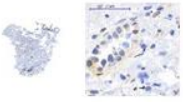

AF_24h